Data Assimilation Experiment of a Heavy Rainfall at Nerima / Tokyo

Hiromu Seko, Takuya Kawabata (MRI/JMA),
Tadashi Tsuyuki (NPD/JMA)

Key factors of generation and development of the convections:

1. Low-level convergence : Doppler-radar, wind-profiler etc.
2. Moist air supply : Sonde, GPS, SSM/I, TMI etc.

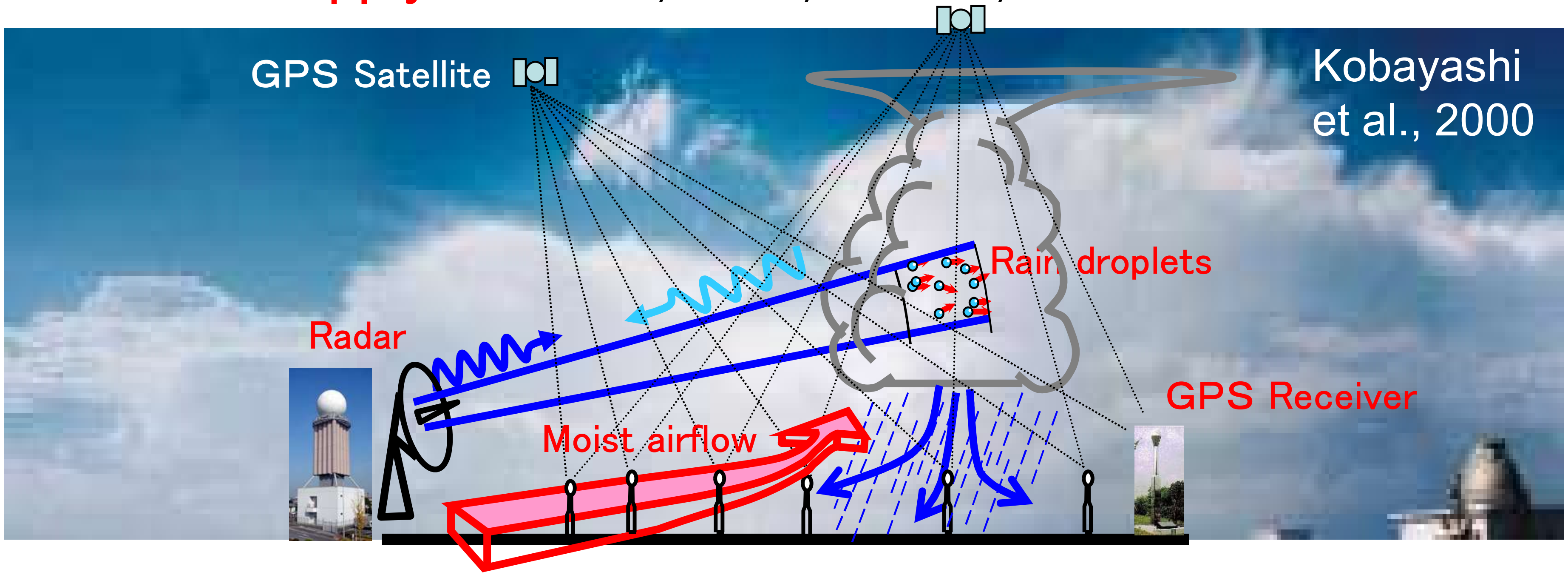

Nerima heavy rainfall on 21 July 1999

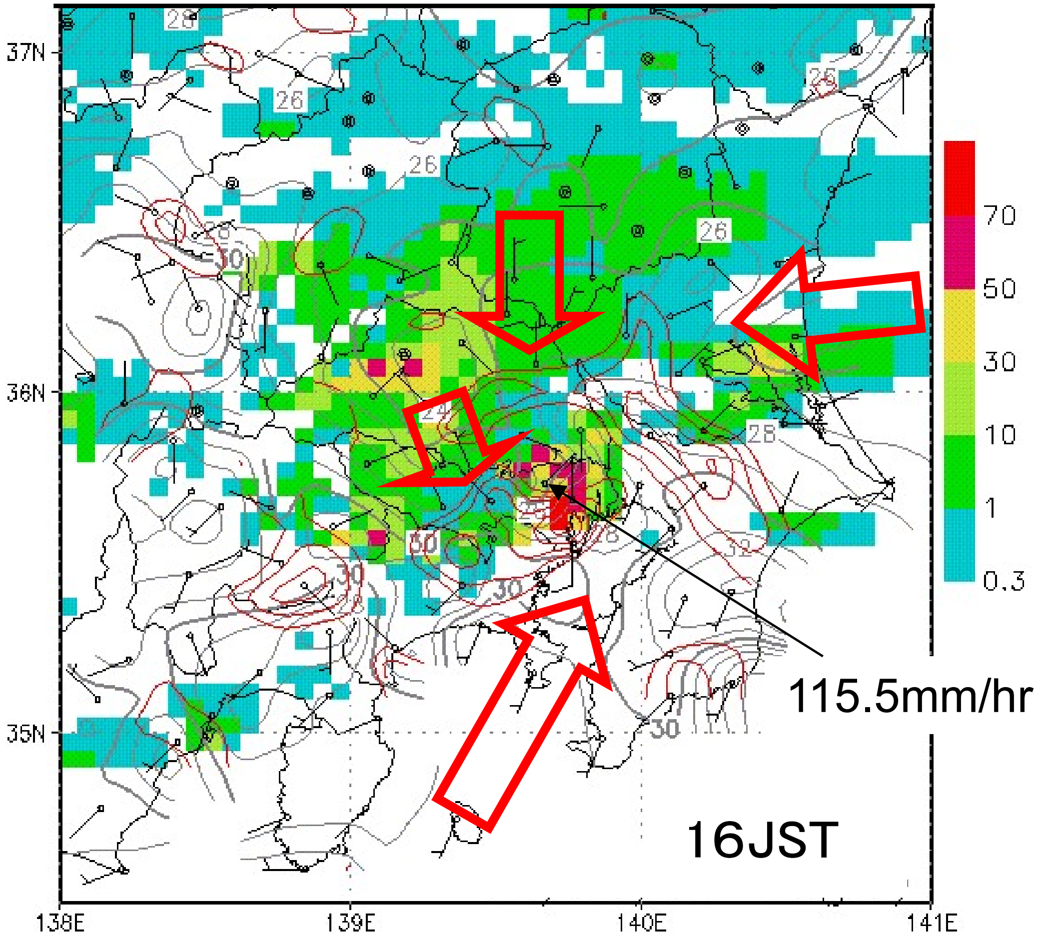

Hourly precipitation amount, temperature (grey line) and convergence (red line) at 16JST

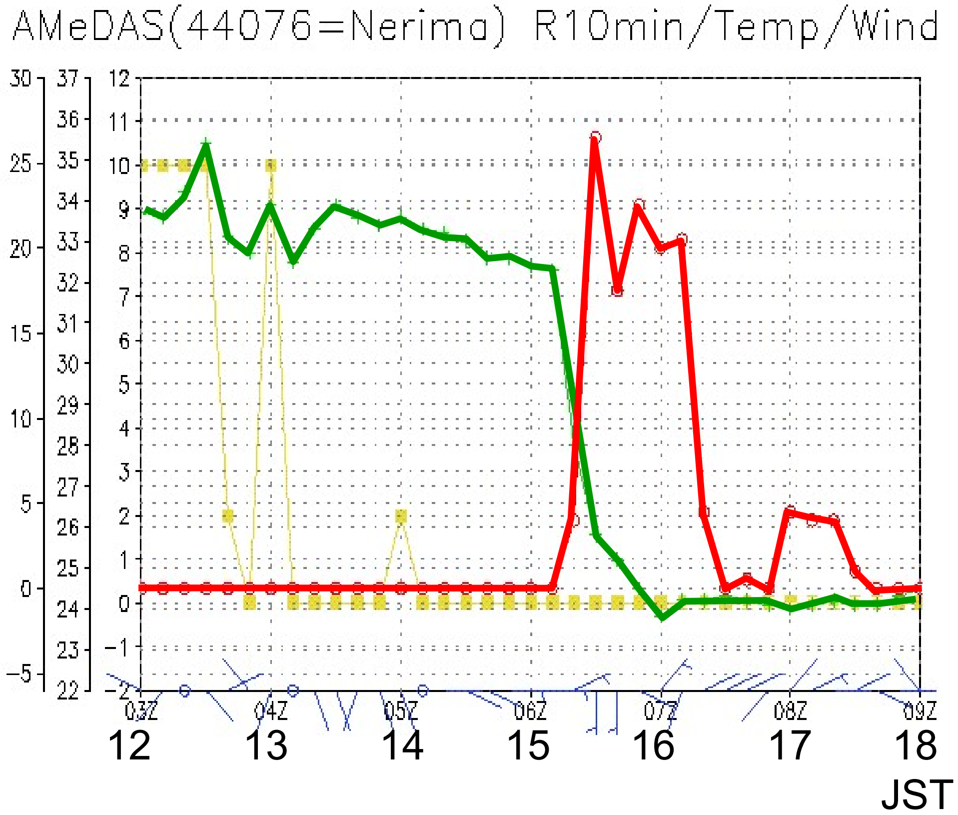

Red: Precipitation

Green : temperature

Yellow : Sun shine

Hourly precipitation of 115.5mm was observed at Nerima, Tokyo

Nerima heavy rainfall on 21 July 1999

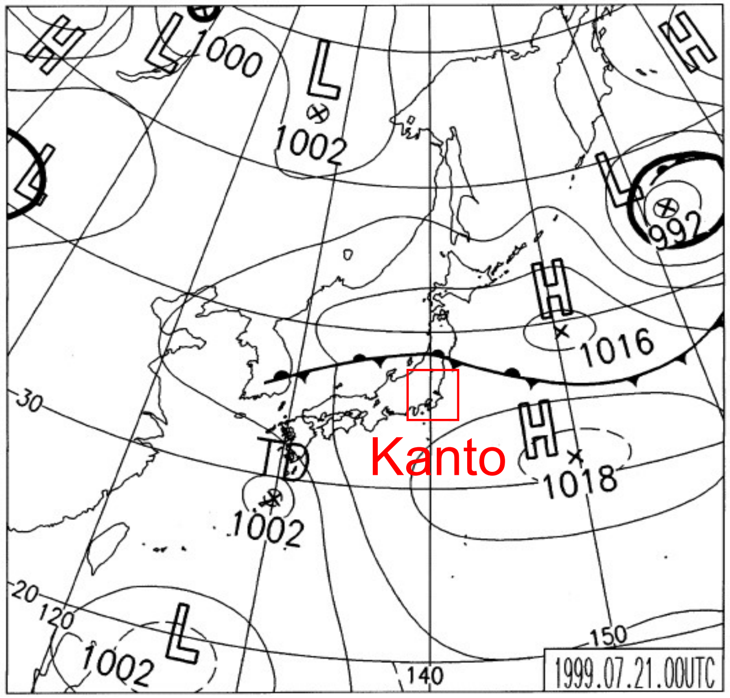

Surface weather chart at 09JST 7/21
(09JST=00UTC)

- Baiu front crossed the northern part of Japan at 09JST.
- Precipitation region of Baiu front moved southward and reached Kanto region at 15JST.

Precipitation observed by operational radars 09–21JST 7/21

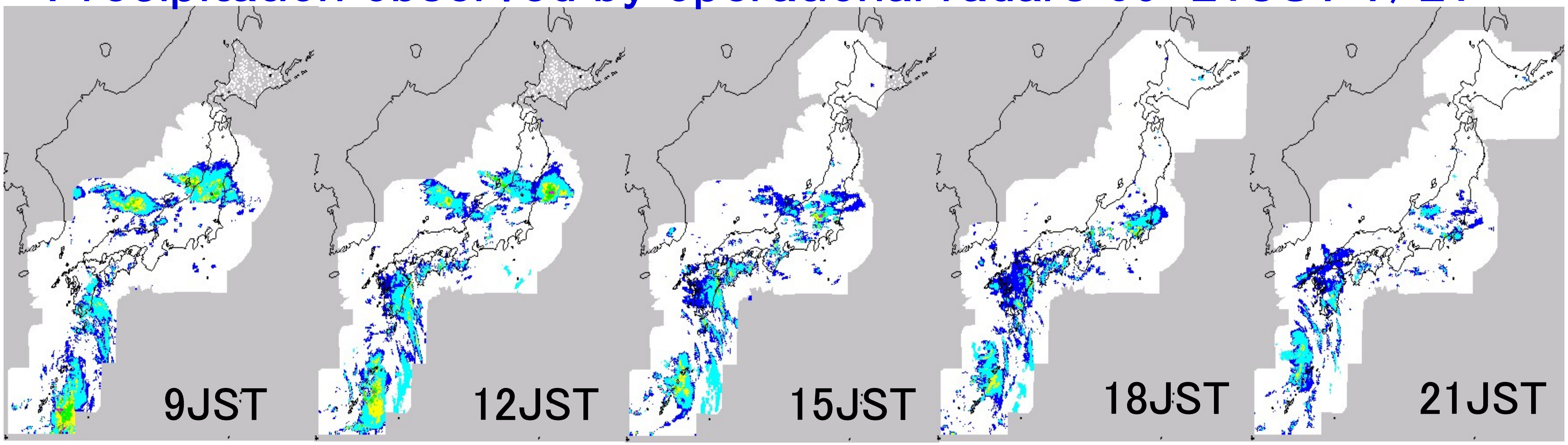

Reflectivity fields and horizontal wind

Reflectivity (dBZ) of Haneda airport radar and horizontal wind at z=1km and 4km obtained by Dual radar analysis

z=4km

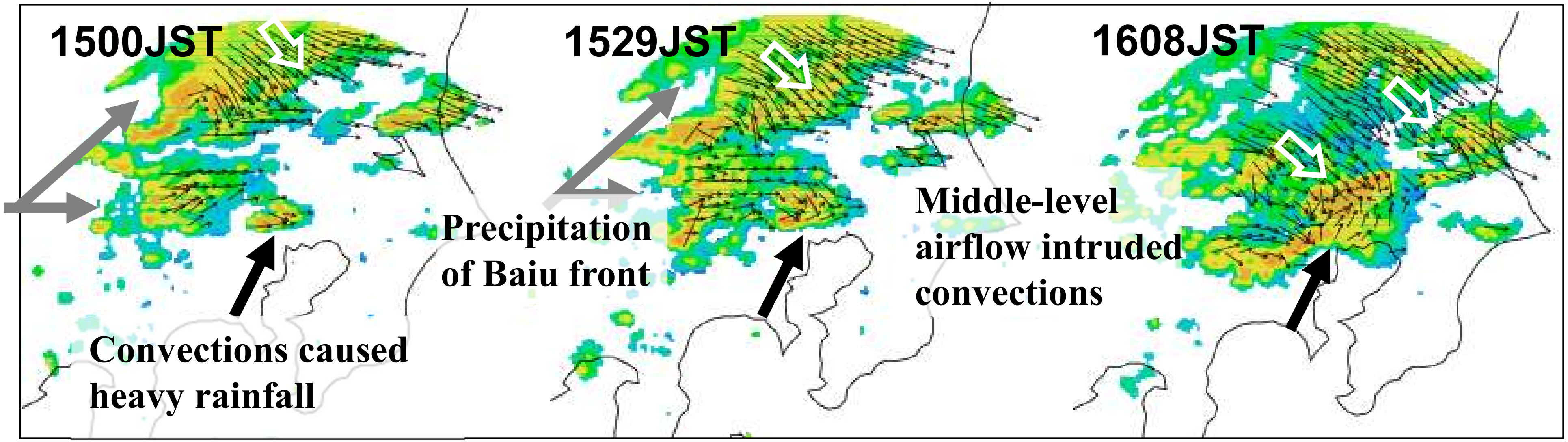

z=1km

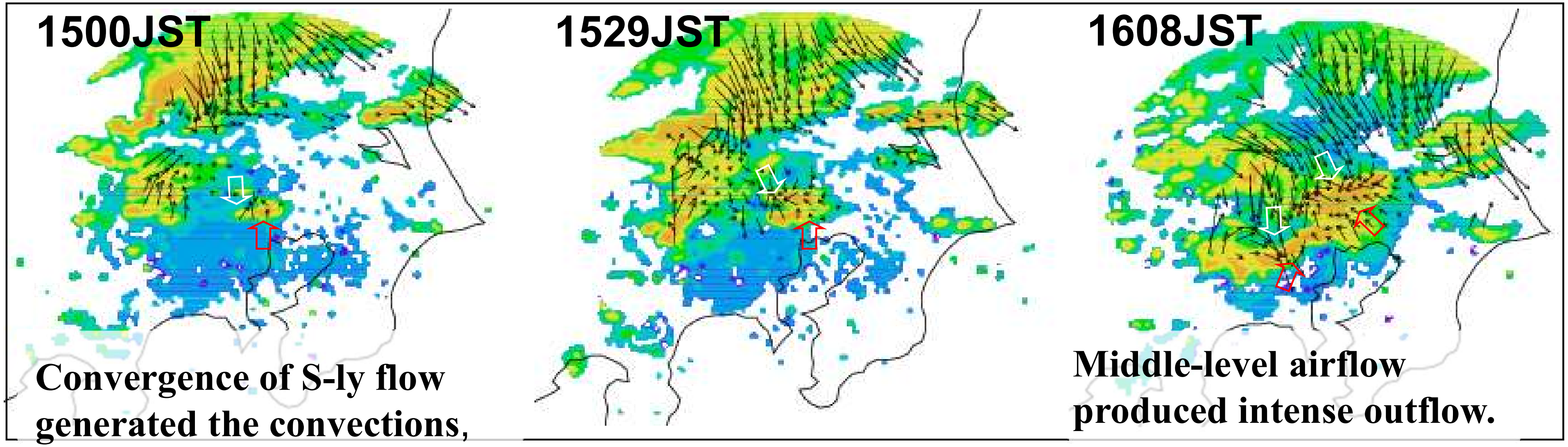

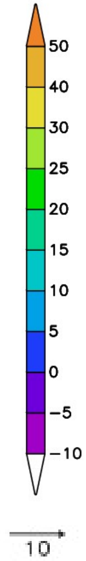

GPS-derived PWV

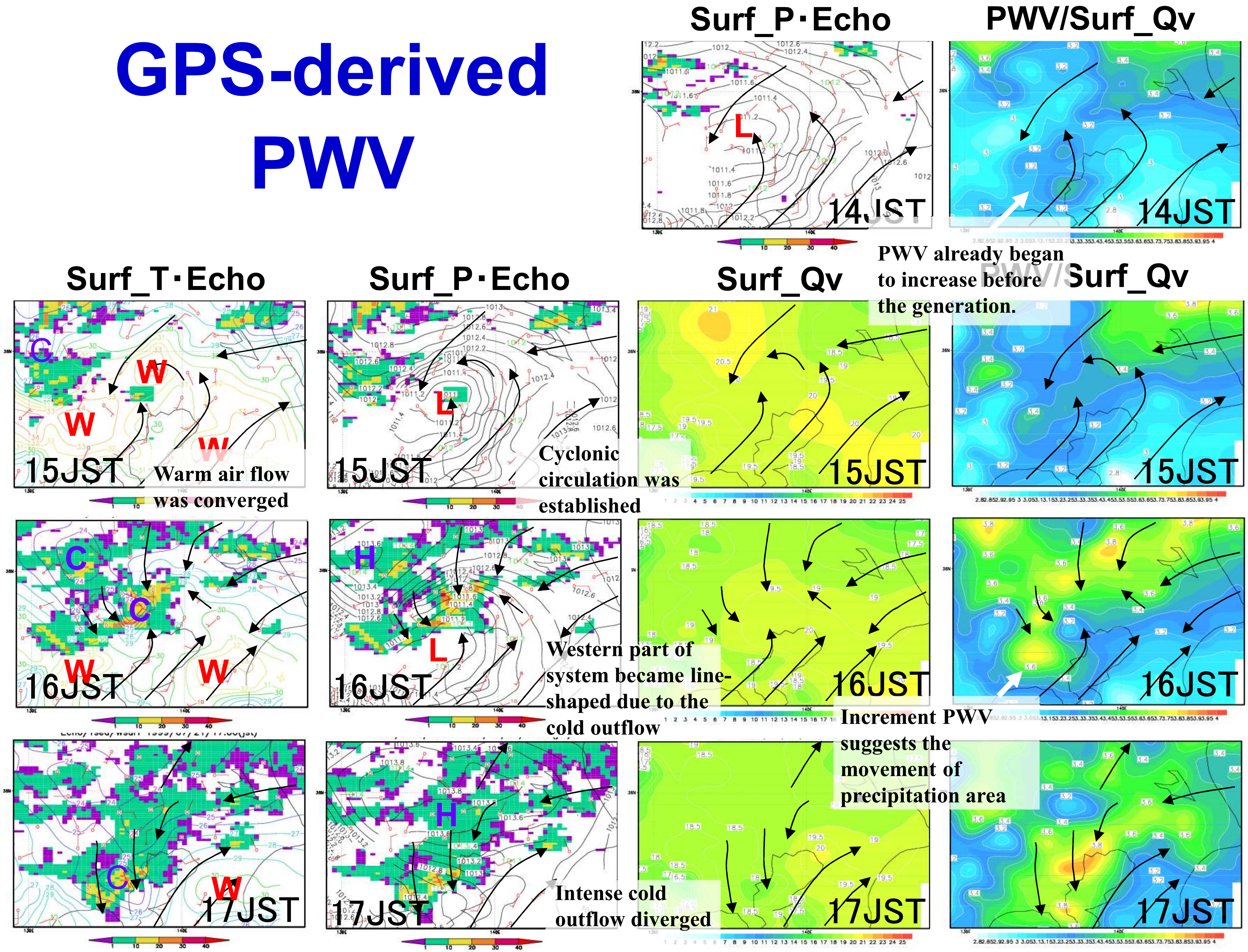

Radial wind data

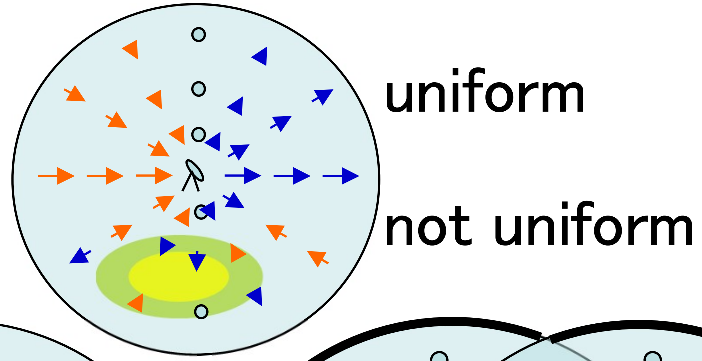

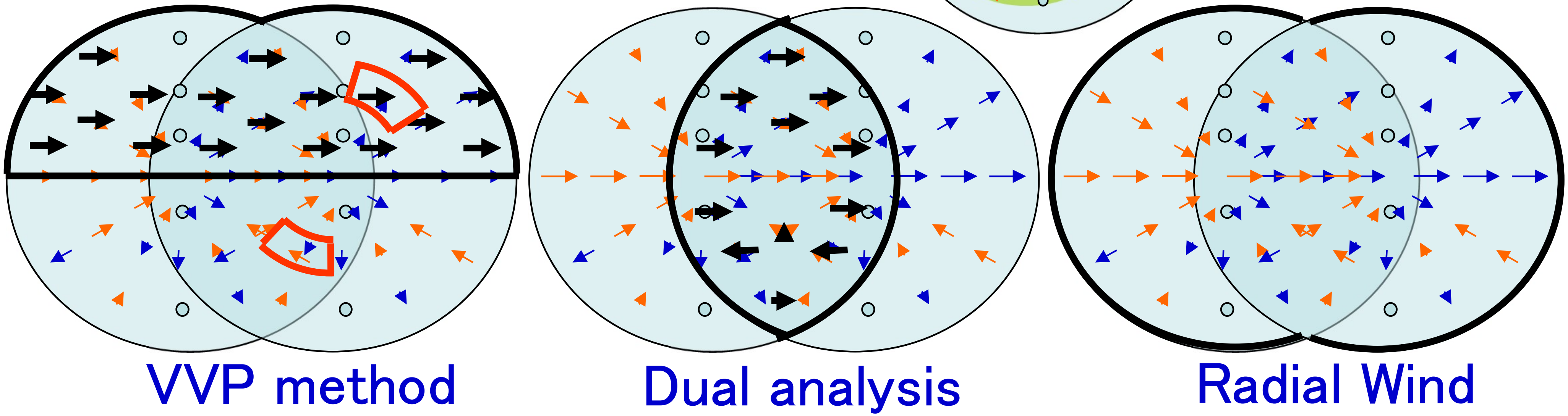

Area where the horizontal wind is estimated:

1. VVP method

   Area, where the horizontal wind can be assumed to be varied uniformly, in whole range of a radar

2. Dual analysis

   Part of area where the ranges of more than two radars are overlapped.

<u>These areas are smaller than whole range of radars.</u>

Doppler radar radial wind data

Vr (Haneda15JST)

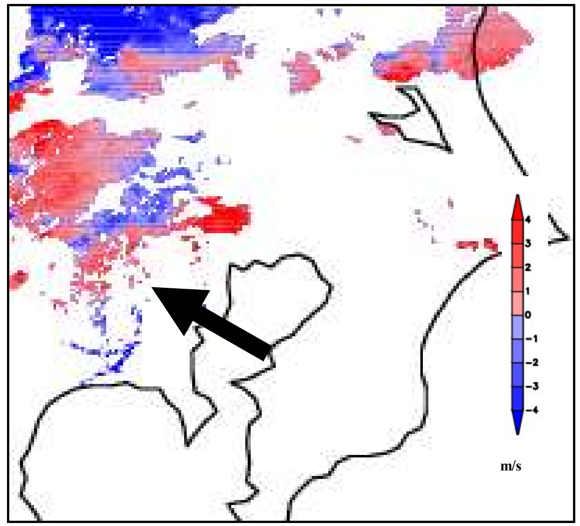

Super observation method

Number of raw data >> number of model grid points.

Radial wind data:

Positions : Grid positions of numerical models on each elevation cone.

Interpolation method : Cressman method.

Range for one data : raw data on the cone within the range of the model grids during 10min before each hours.

$$Vr\_obs = \sum_{x=x_0-\Delta x/2}^{x_0+\Delta x/2} \sum_{y=y_0-\Delta y/2}^{y_0+\Delta y/2} w Vr \Big/ \sum_{x=x_0-\Delta x/2}^{x_0+\Delta x/2} \sum_{y=y_0-\Delta y/2}^{y_0+\Delta y/2} w$$

$$w = \frac{R^2 - D^2}{R^2 + D^2}$$

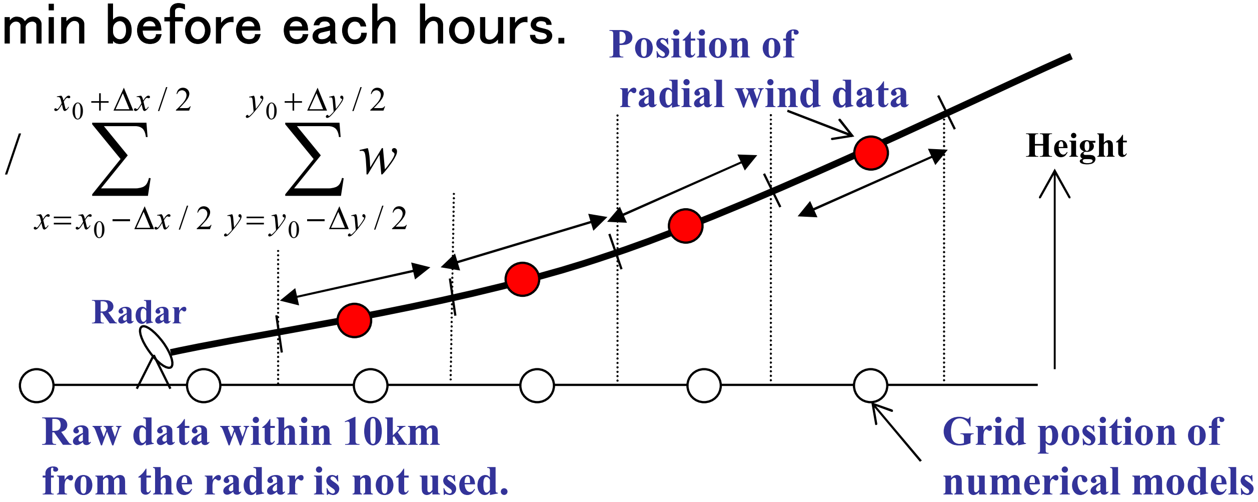

where, D is distance between the radial wind data point and raw data.

R is set to 5km.

Elevation range : 0.0 – 5.4 deg. (where the vertical velocity can be neglected)

Observation operator

Simulated radial wind were estimated from grid point values with the weight of the radar beam intensity.
(It is assumed that radar beam intensity has Gauss distribution.)

$$Vr\_model = \sum_{x=x_0-\Delta x/2}^{x_0+\Delta x/2} \sum_{y=y_0-\Delta y/2}^{y_0+\Delta y/2} \sum_{\theta=\theta_{beam}-1^\circ}^{\theta_{beam}+1^\circ} w\, Vr\_grid \Bigg/ \sum_{x=x_0-\Delta x/2}^{x_0+\Delta x/2} \sum_{y=y_0-\Delta y/2}^{y_0+\Delta y/2} \sum_{\theta=\theta_{beam}-1^\circ}^{\theta_{beam}+1^\circ} w$$

$$w = \frac{R^2 - D^2}{R^2 + D^2} \times e^{-\left(\frac{\theta_{gridl}-\theta_{beam}}{\theta_h}\right)^2 \log_e 2}$$

$$\theta_h = 1.27\lambda / A / 2 \quad (rad)$$

where、
R : radius of influence,
D : distance between model grids and radial wind data,
A : Diameter of antenna.

Beam cut due to the mountains is taken into consideration.

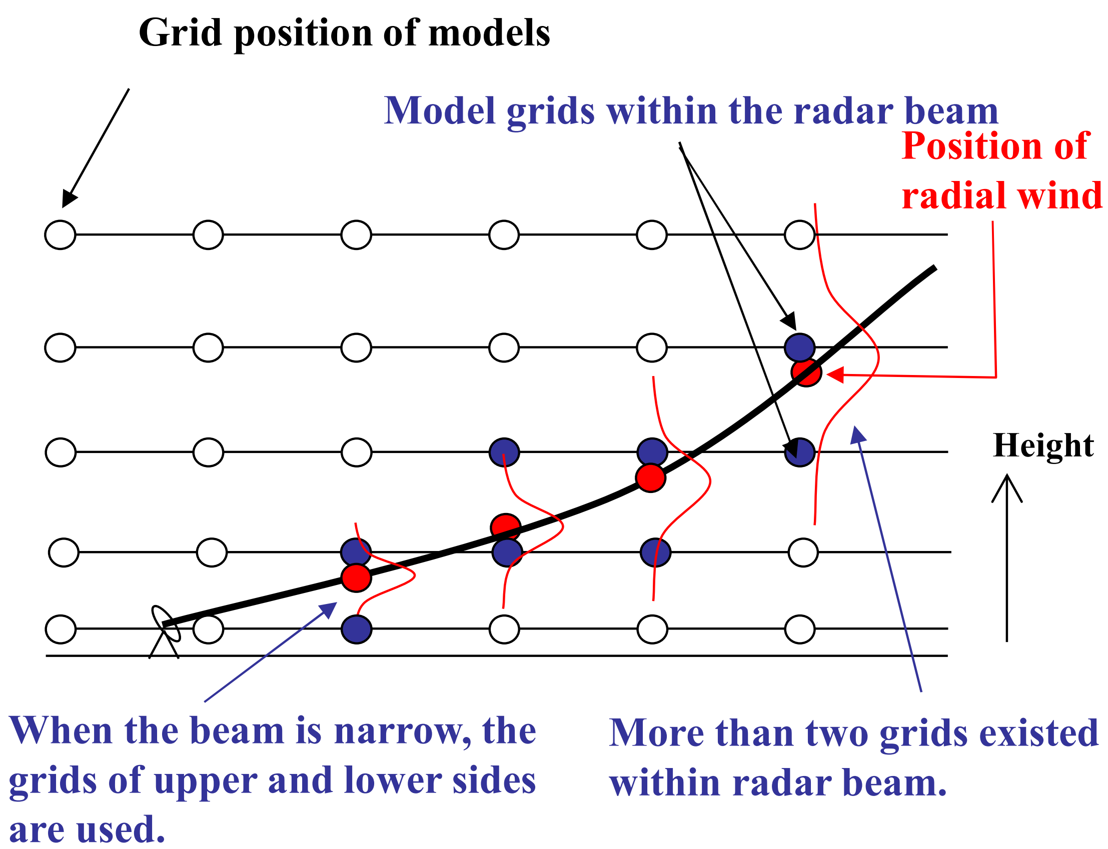

GPS water vapor data

- Phase delay of signals (slant delay) was obtained from GEONET data.
- Precipitable water vapor (PWV) and Slant water vapor (SWV) were estimated from slant delay with surface pressure and temperature.
- Influence of Multipath and PCV was removed (Iwabuchi et al.2004; Shoji et al. 2004).

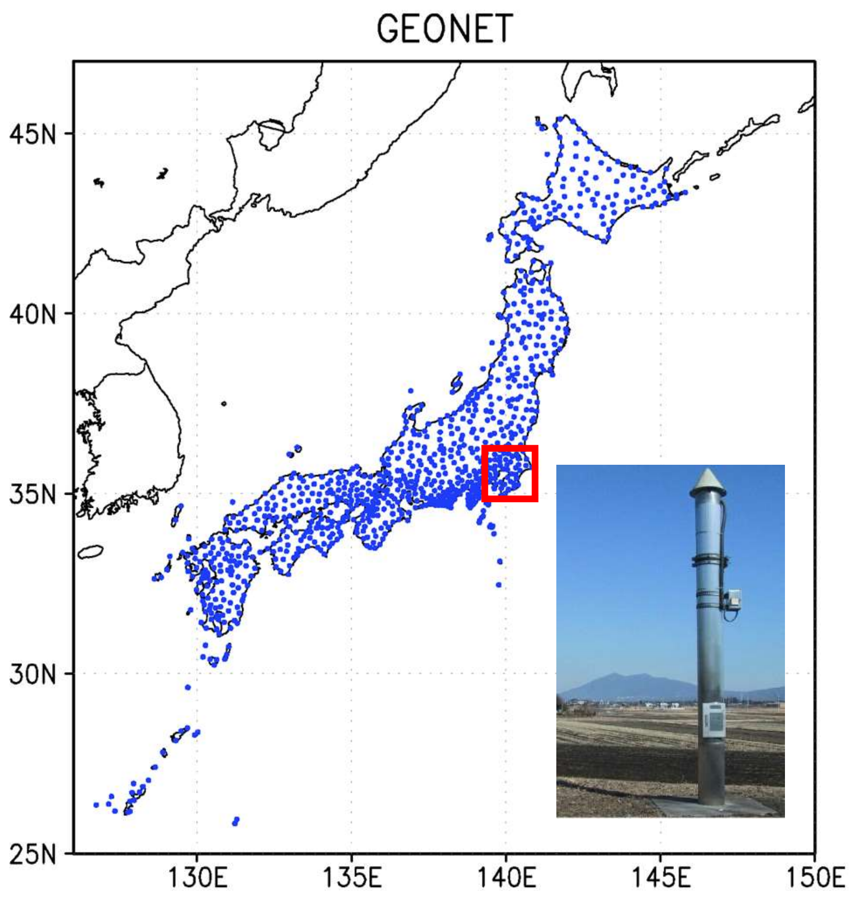

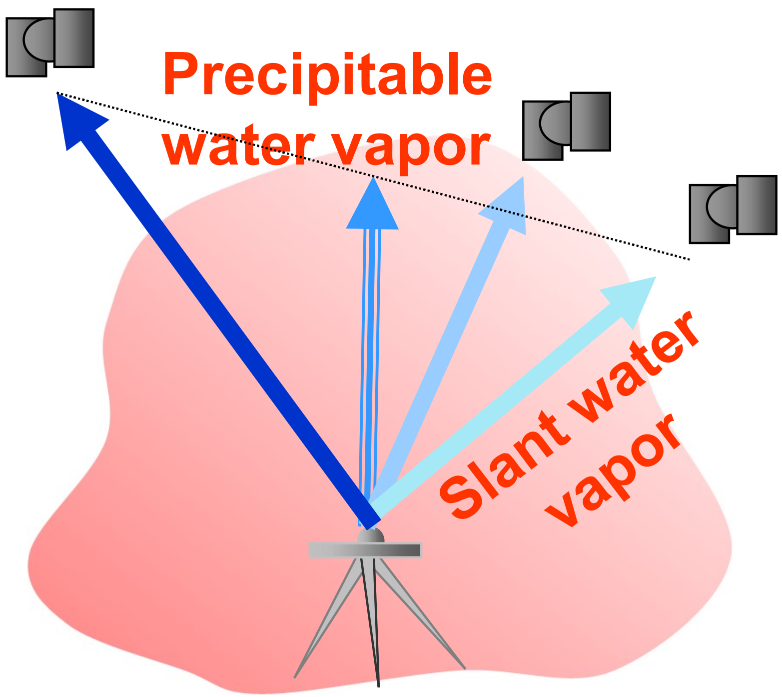

SWV has information of 3D water vapor distribution.

GPS water vapor data

- Phase delay of signals (slant delay) was obtained from GEONET data of GSI.
- Precipitable water vapor (PWV) and Slant water vapor (SWV) were estimated from slant delay with surface pressure and temperature.

Observation operator

- Path was traced from GPS receiver positions by the ray tracing method.
- Density ρ and specific humidity q_v were estimated by Cressman interpolation method.
- SWV is estimated by integration of $\rho \times q_v$.

$$Swv\_mdl = \sum_{i=1}^{i=i\_top(z=15km)} l_i \, \rho \, q_v$$

- The GPS data of which altitude was less than 50m from the altitude of a model was used.

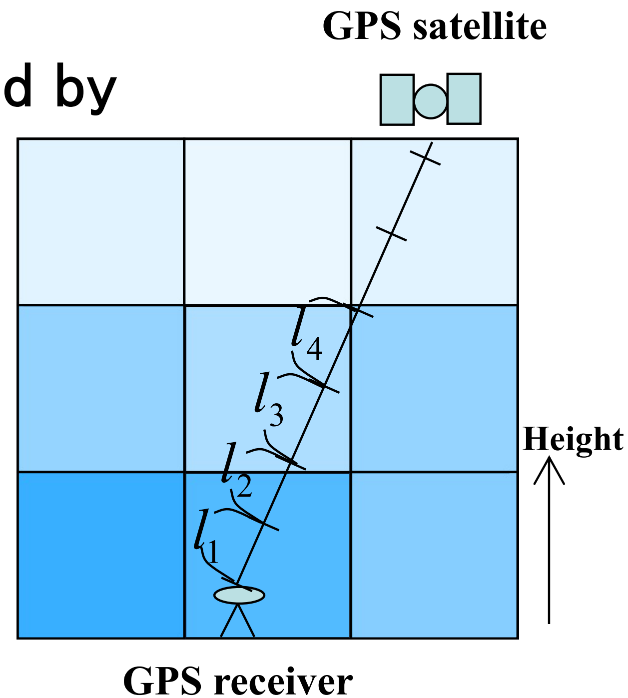

Challenge:

- Precipitation region of Baiu front moved into the ranges of Doppler radars at 15JST
- Conventions at southern Kanto was just generated at 15JST
- We want to reproduce the precipitation at the southern Kanto by using the data from 9JST to 15JST with MSM-4DVar system.

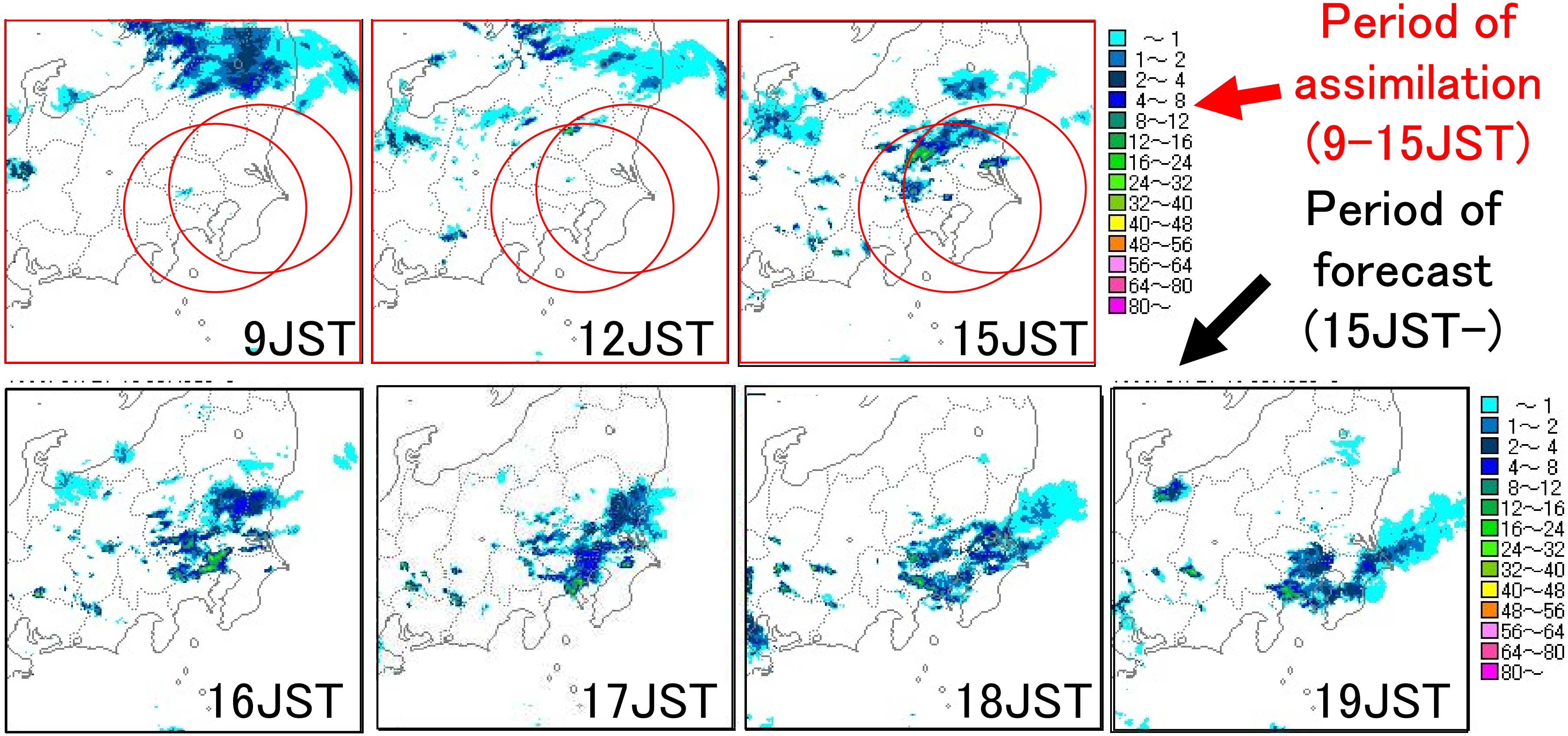

Radar-derived rainfall intensity (1999 7/21 09-21JST)
Circles indicate the range of the Doppler radars

First Guess of MSM 7/21 9-21JST (without assimilation)

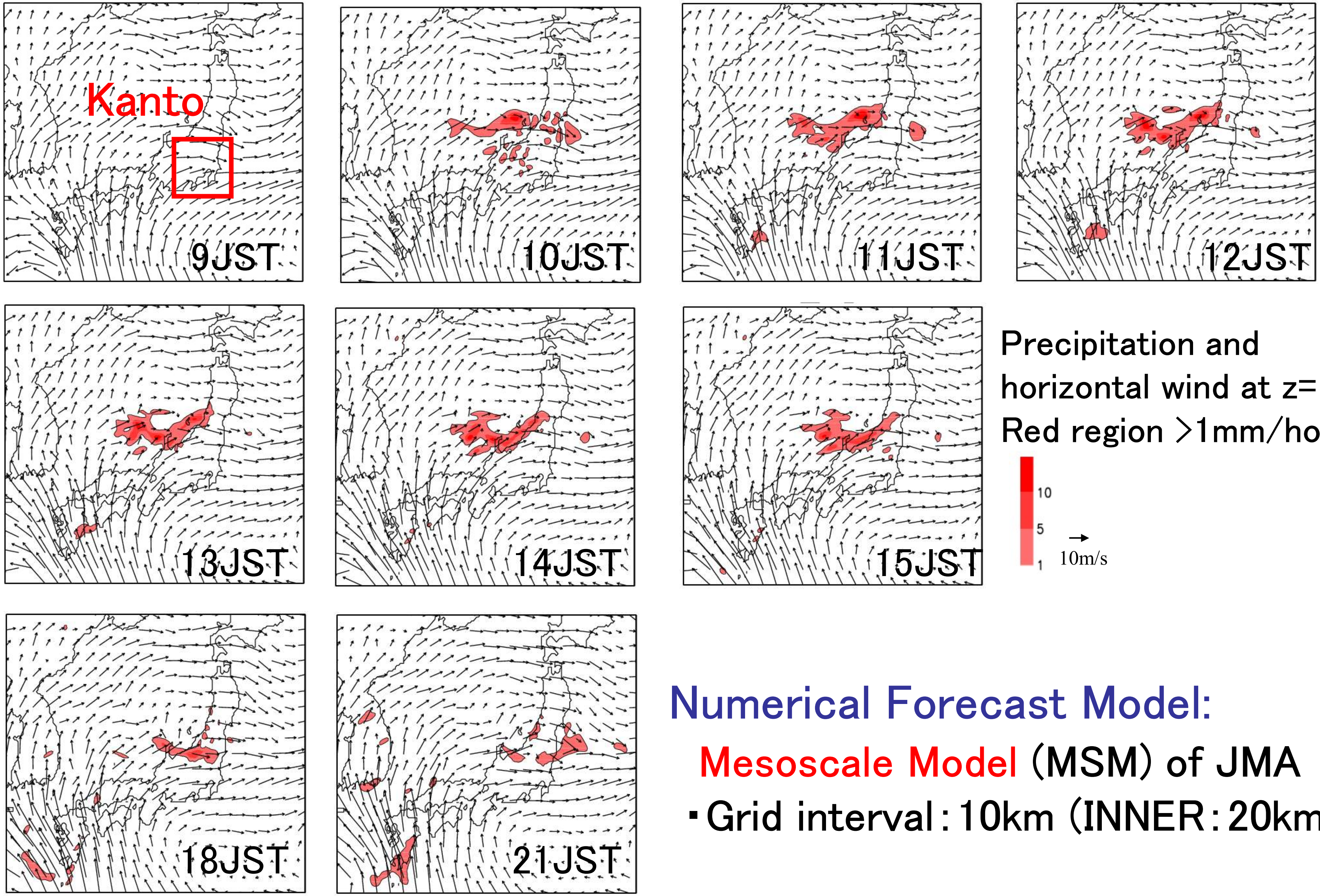

Precipitation and horizontal wind at z=1.5km
Red region >1mm/hour.

Numerical Forecast Model:

Mesoscale Model (MSM) of JMA

- Grid interval : 10km (INNER : 20km)

- Simulated Baiu front stayed north of Kanto (□).

Verification of precipitation（16-18JST）

Hourly precipitation and horizontal wind at z=0.5km

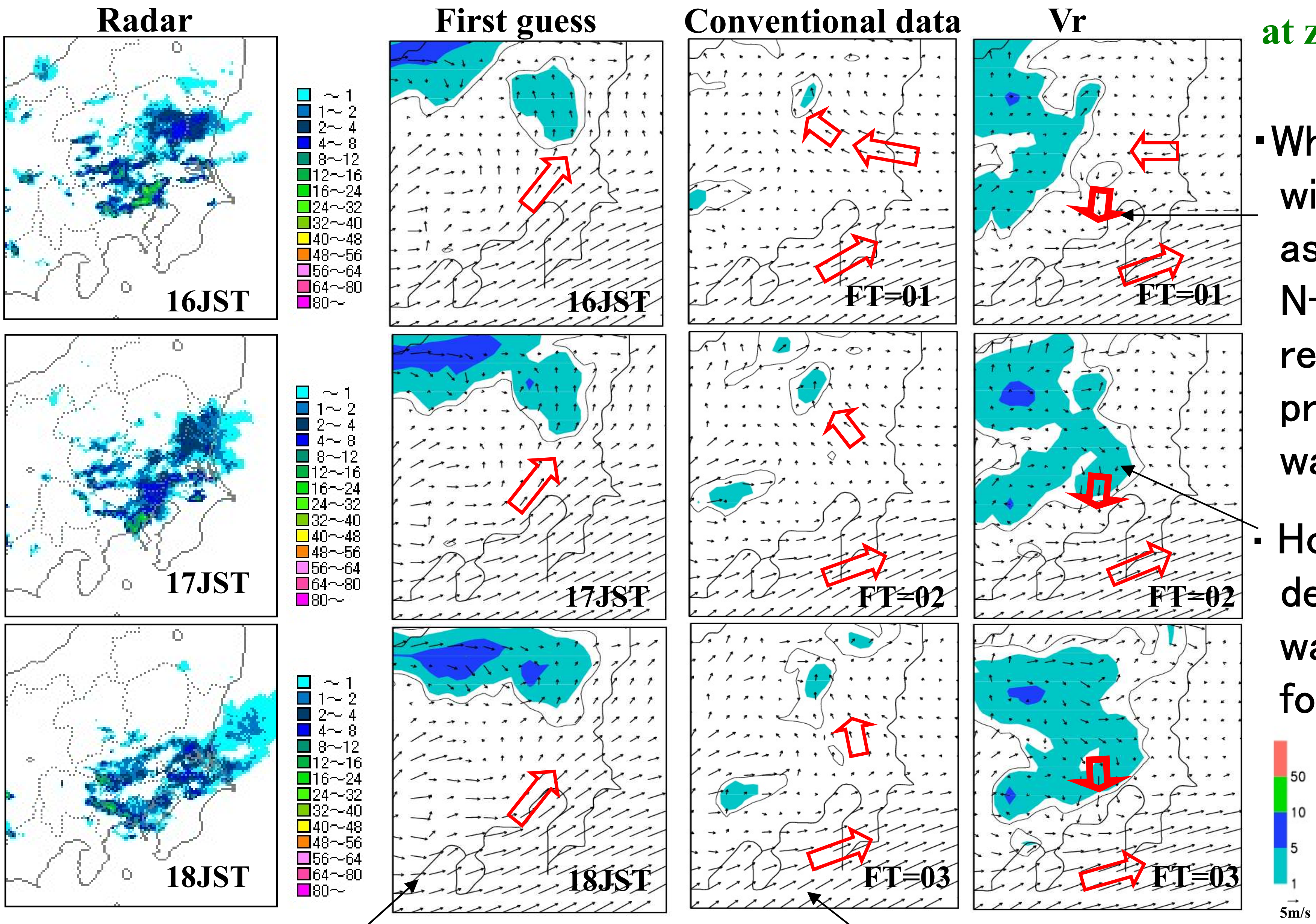

- When the radial wind was assimilated, N-ly wind was reproduced and precipitation was generated.
- However the development was delayed for 1hour.

- When sonde data was assimilated, E-ly flow was simulated. However, precipitation was not reproduced.

- When assimilation was not performed, the southwesterly wind predominated.

Verification of precipitation（16－18JST）

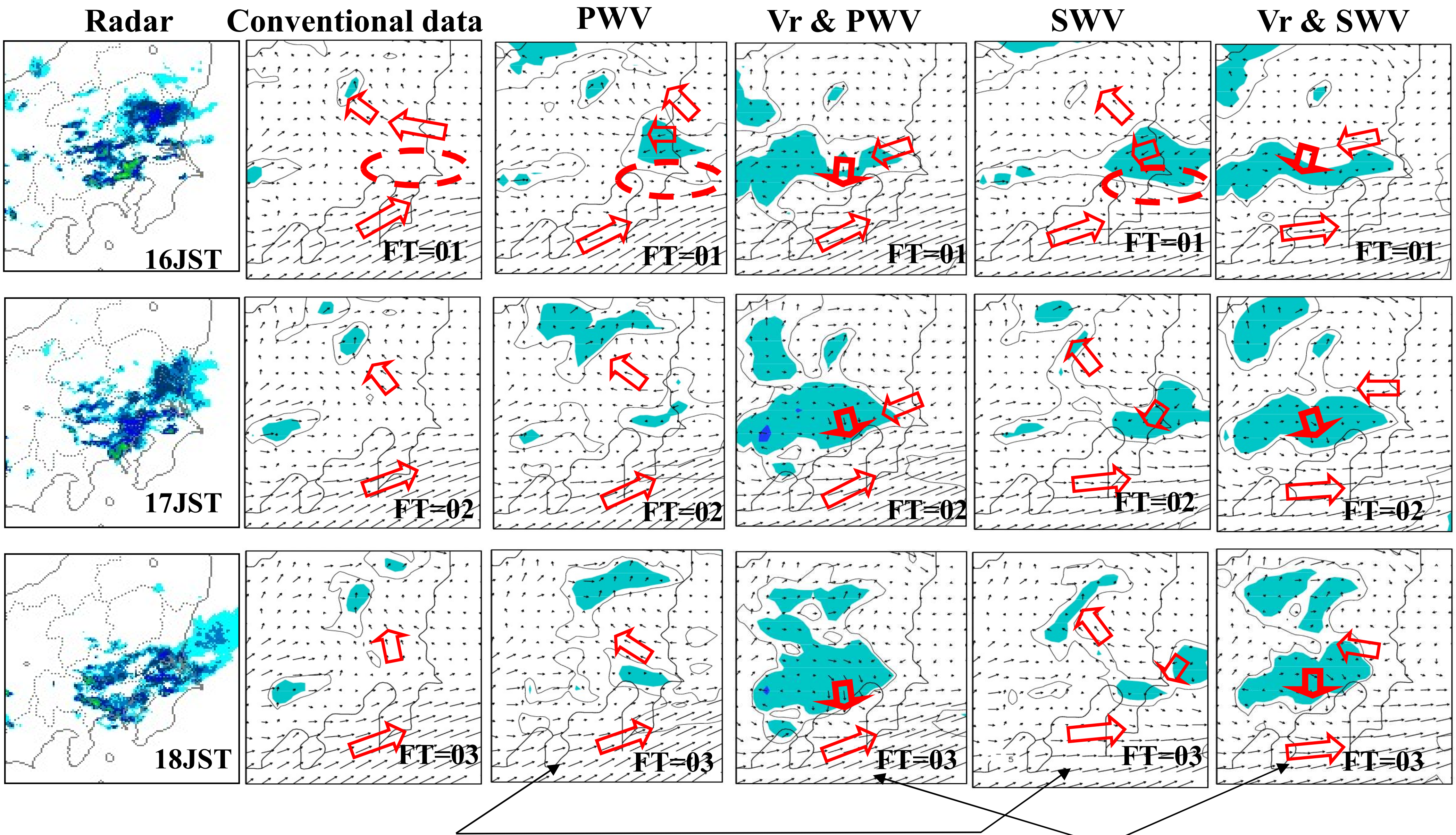

- When GPS data was assimilated, the precipitation was generated. However, its position was shifted to the east.
- When both data were used, the precipitation was generated where it was observed.

Verification of precipitation (16-21JST)

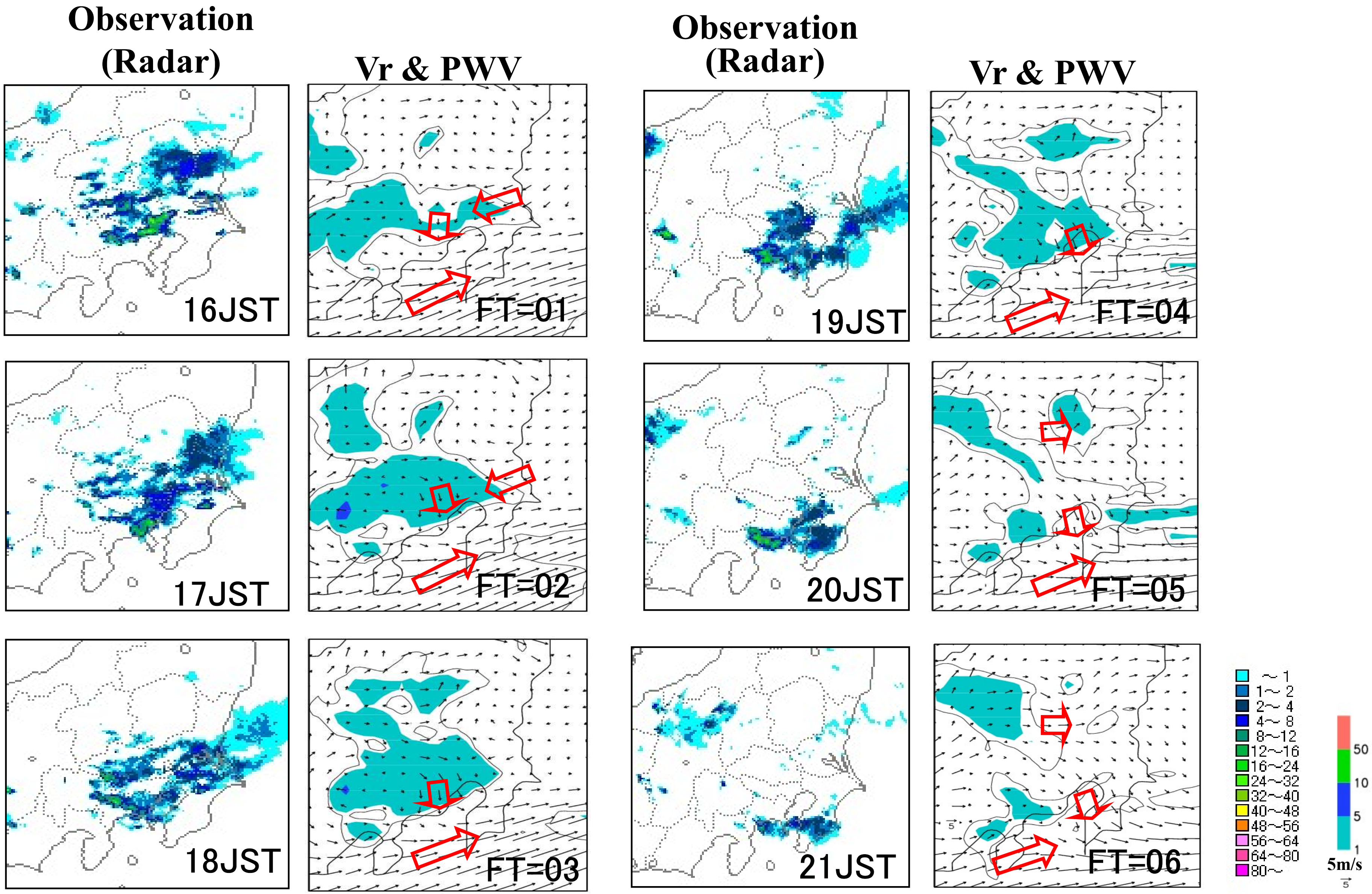

・When Vr and PWV data were used, the precipitation was well reproduced until 21JST (FT=06hr).

Effective height of radial wind data

Hourly precipitation and horizontal wind at z=0.5km

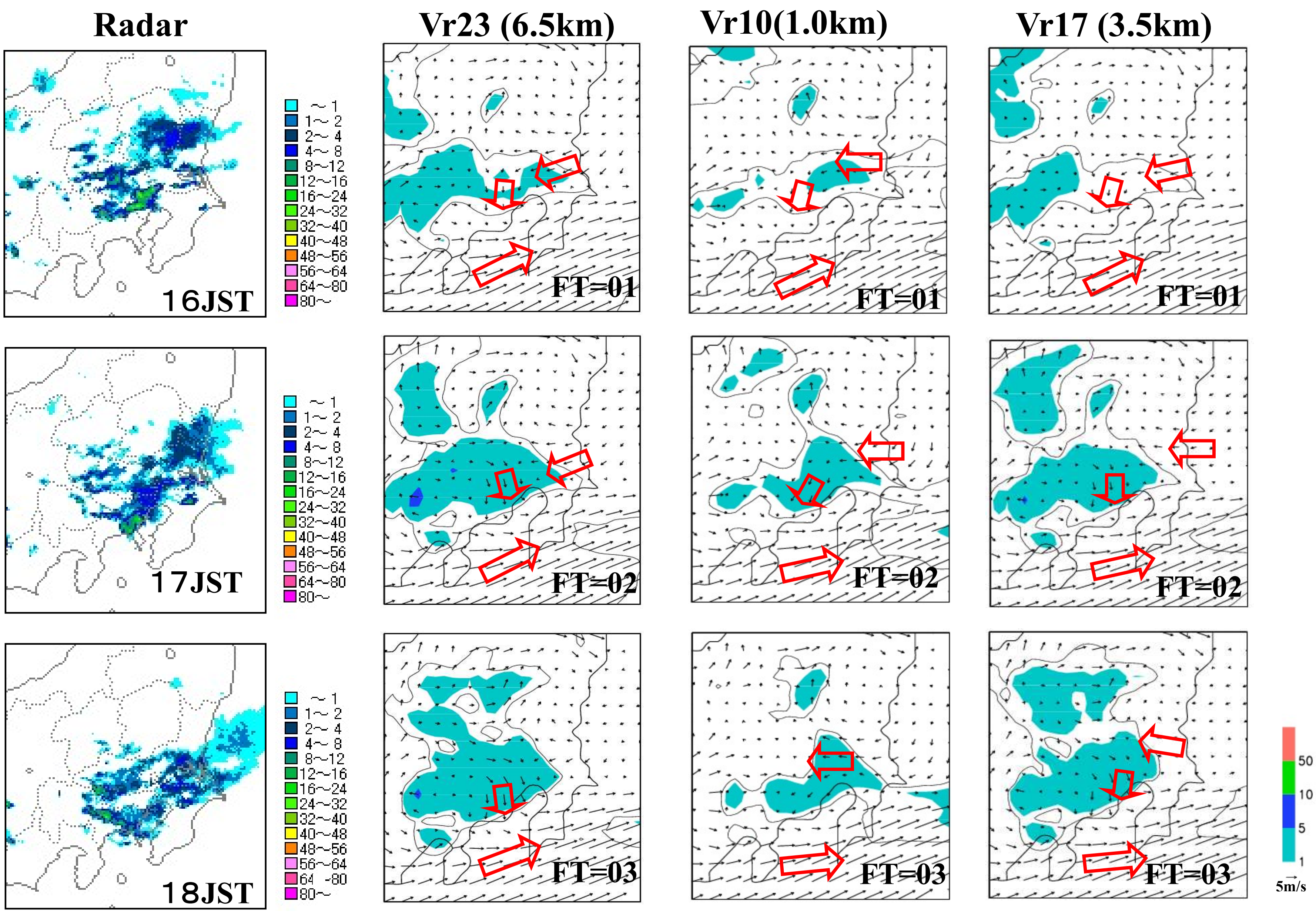

・Even radial wind at z<1km was assimilated, the precipitation. was reproduced.

→ In this case, the low-level flow is important for the generation of the precipitation

Influence of the radial wind range

Hourly precipitation and horizontal wind at z=0.5km

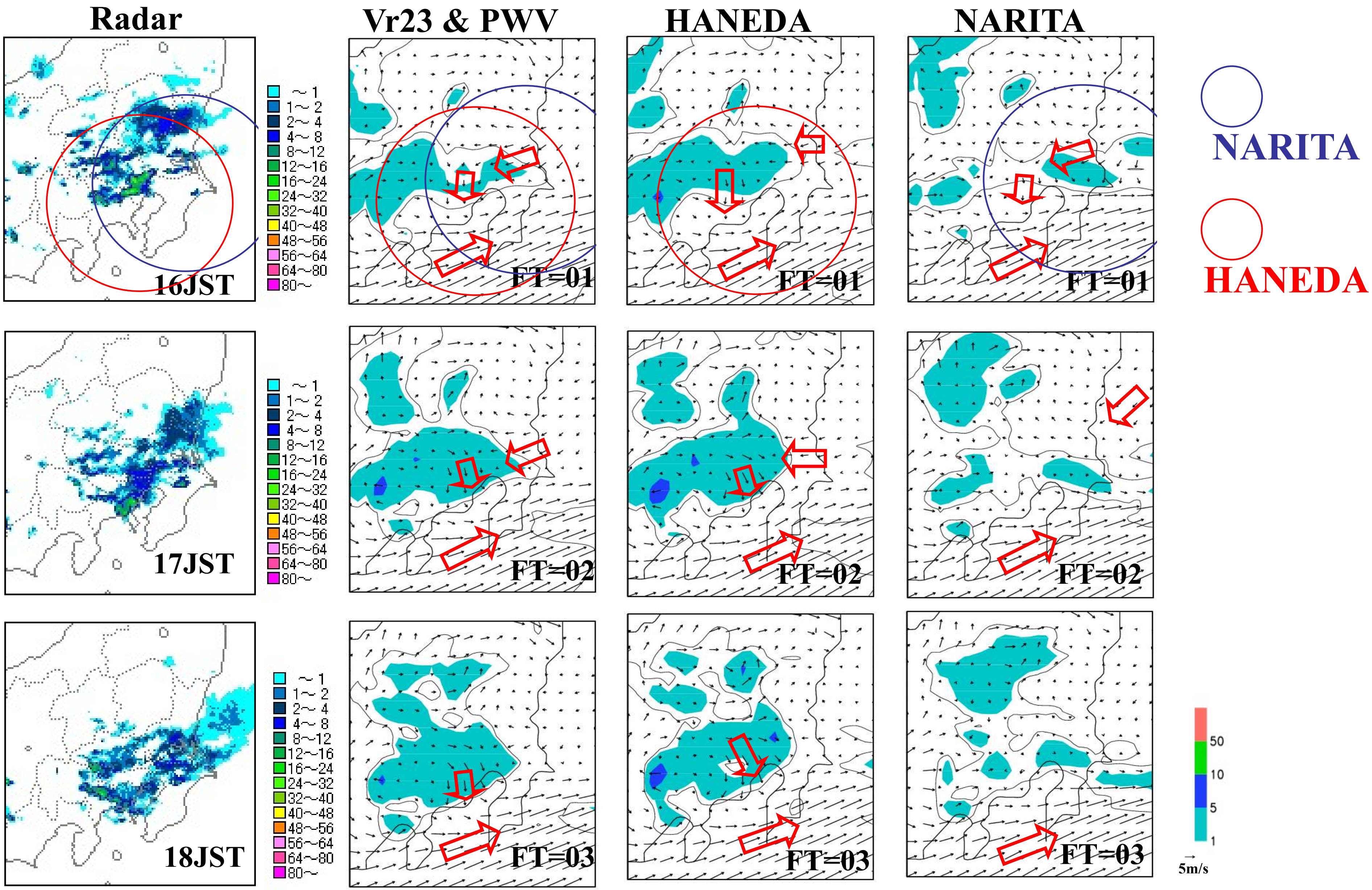

・N-ly wind was reproduced by low-level radial wind observed by HANEDA radar.
(NARITA data can not detect N-ly flow that existed below the cone of lowest elevation.)
→ It also indicates the importance of the low-level flow.

Surface wind and water vapor of analyzed fields

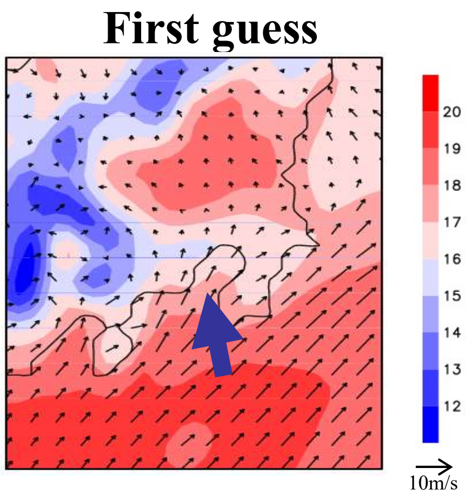

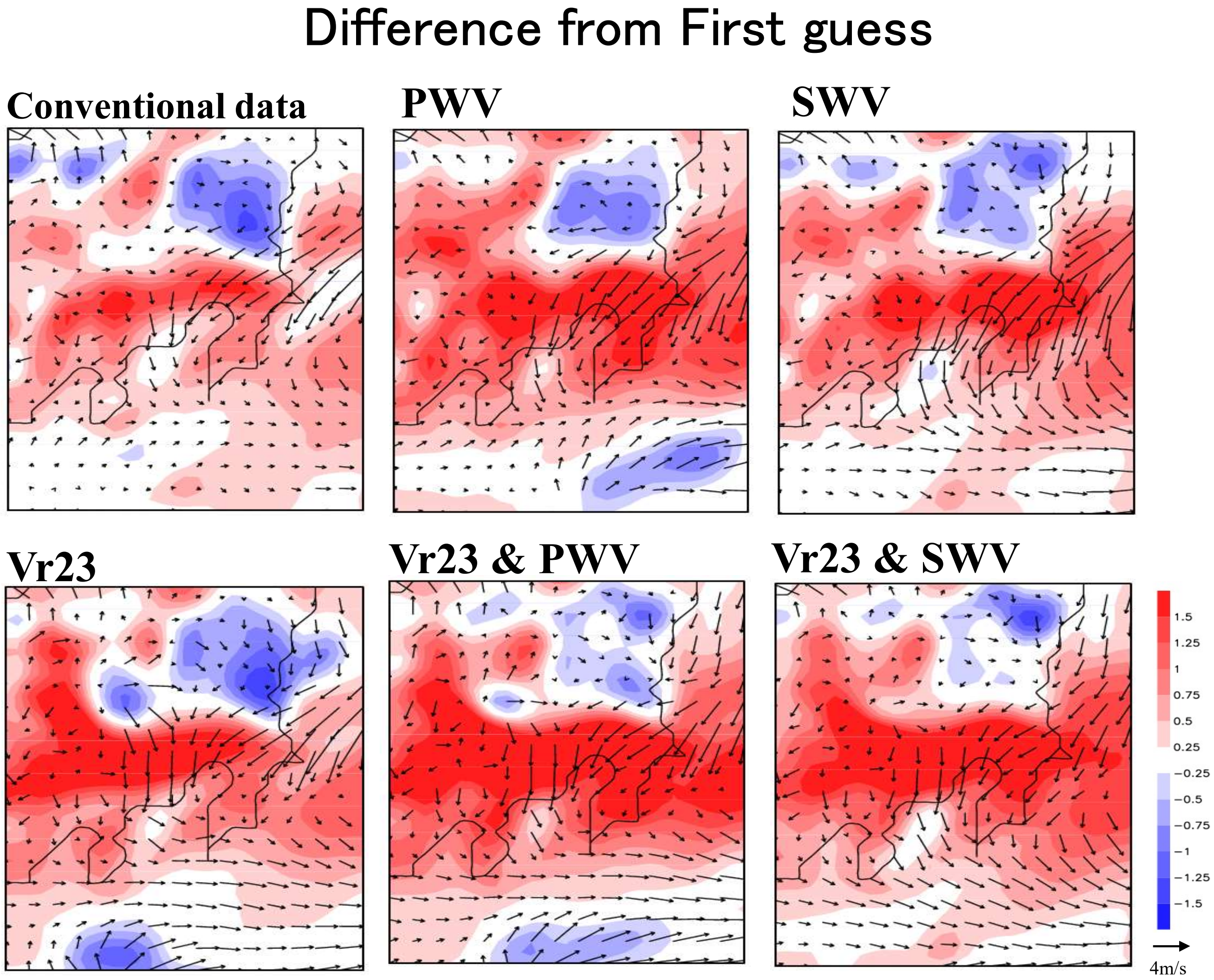

- On the southern part of Kanto (➡), low water vapor region existed
- In all experiments, water vapor of southern Kanto is increased.

- S-ly flow was weakened where water vapor increased.
  →This change of the horizontal wind intensifies the low-level convergence and moves the convergence southward.

Surface wind and water vapor of analyzed fields

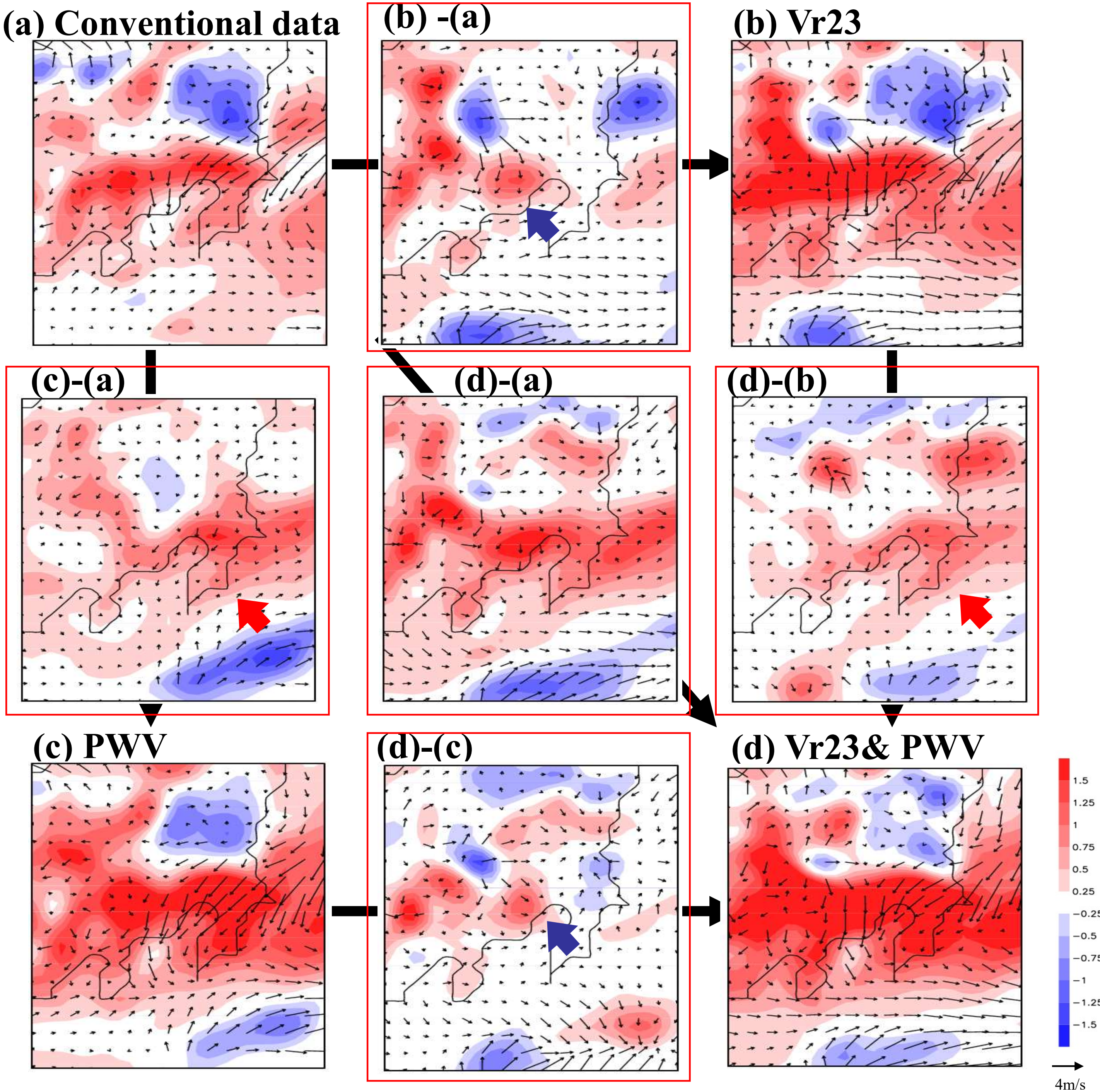

- Radial wind (GPS water vapor) increases the water vapor at southwest (➡) (southeast(➡)) part of Kanto.
- The difference between each experiment indicates the influence of radial wind and GPS data.
- Difference indicates the following relation;
  Convergence – Increase
  Divergence – Decrease
  →
  - Water vapor changes the horizontal wind.
  - Horizontal wind changes the water vapor distribution.

First guess

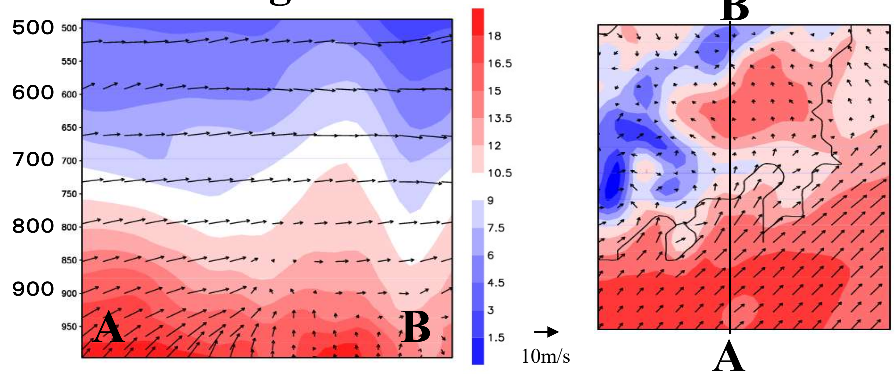

Benefit of SWV data
(N-S cross sections of analyzed water vapor)

Difference from first guess
(water vapor and horizontal wind)

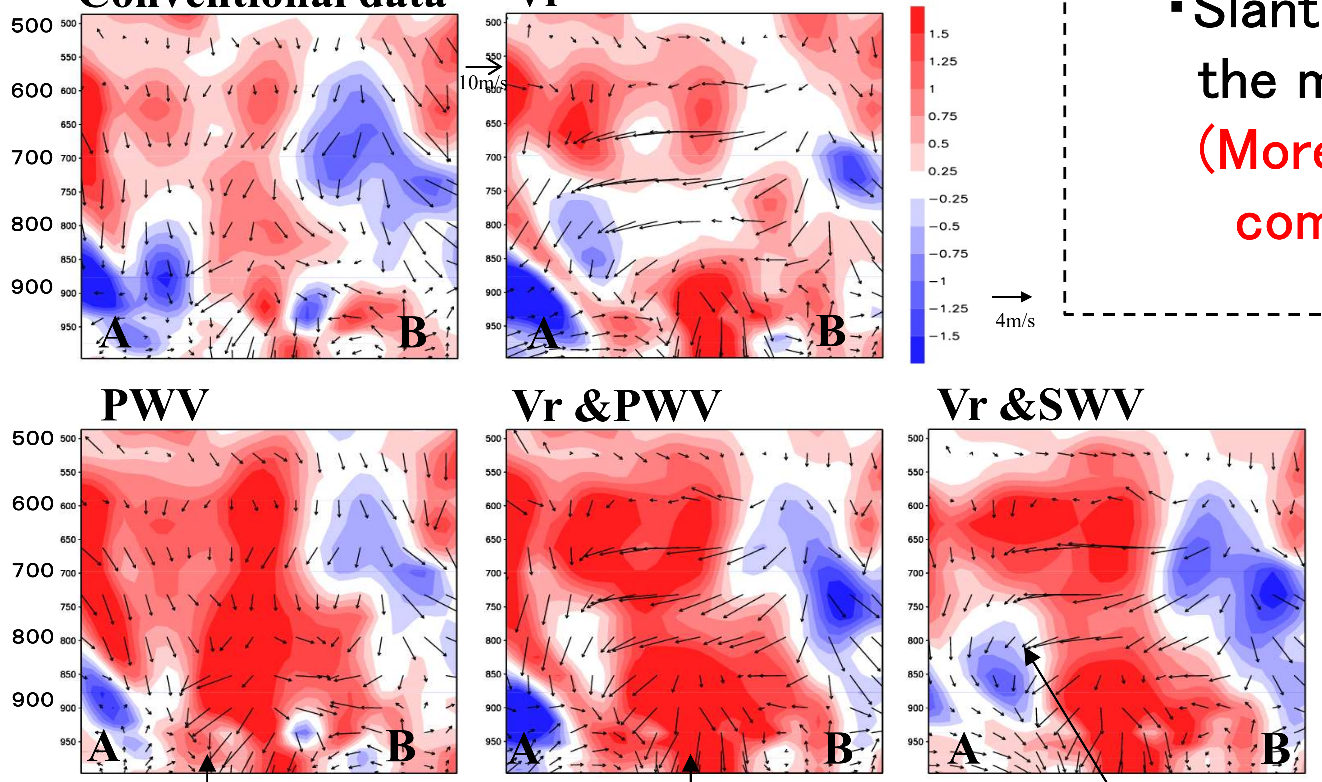

- PWV increases the water vapor at whole layers.
- Slant water vapor decreases the middle-level water vapor. (More realistic distribution, compared with PWV case)

Effect of slant paths
Vr&SWV-Vr&PWV

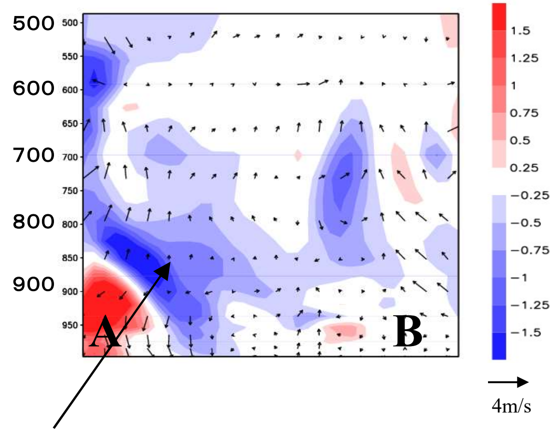

PWV increased the water vapor with keeping their vertical features.

Slant data decreased the middle-level water vapor.

Verification of precipitation (16-21JST)

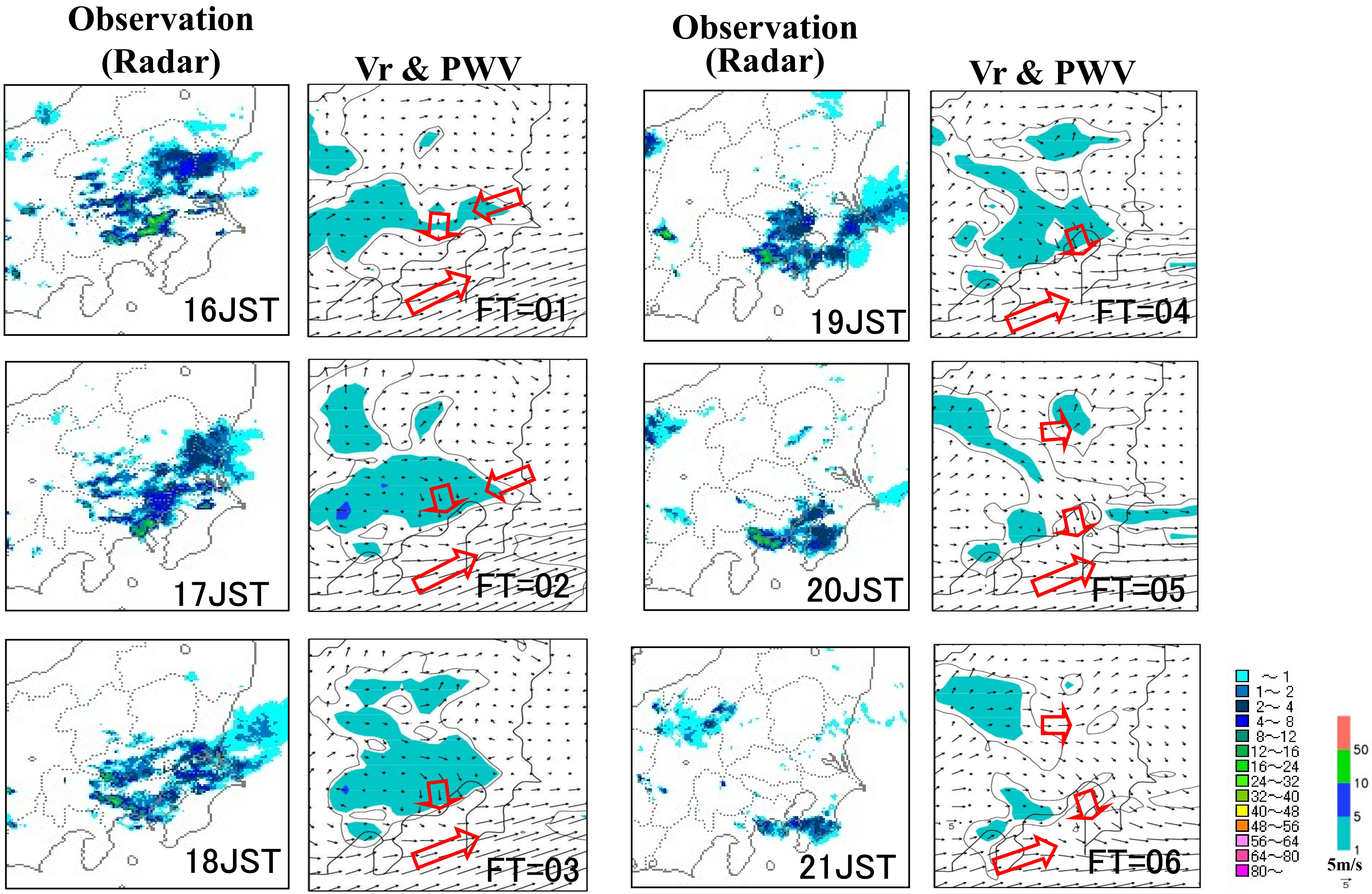

- Precipitation was well reproduced until 21JST (FT=06hr).
- To reproduce the intensity,
  PWV and Vr were assimilated into NHM by 3DVar system.

NHM-3DVar

NHM-3dvar analysis fields from first guess

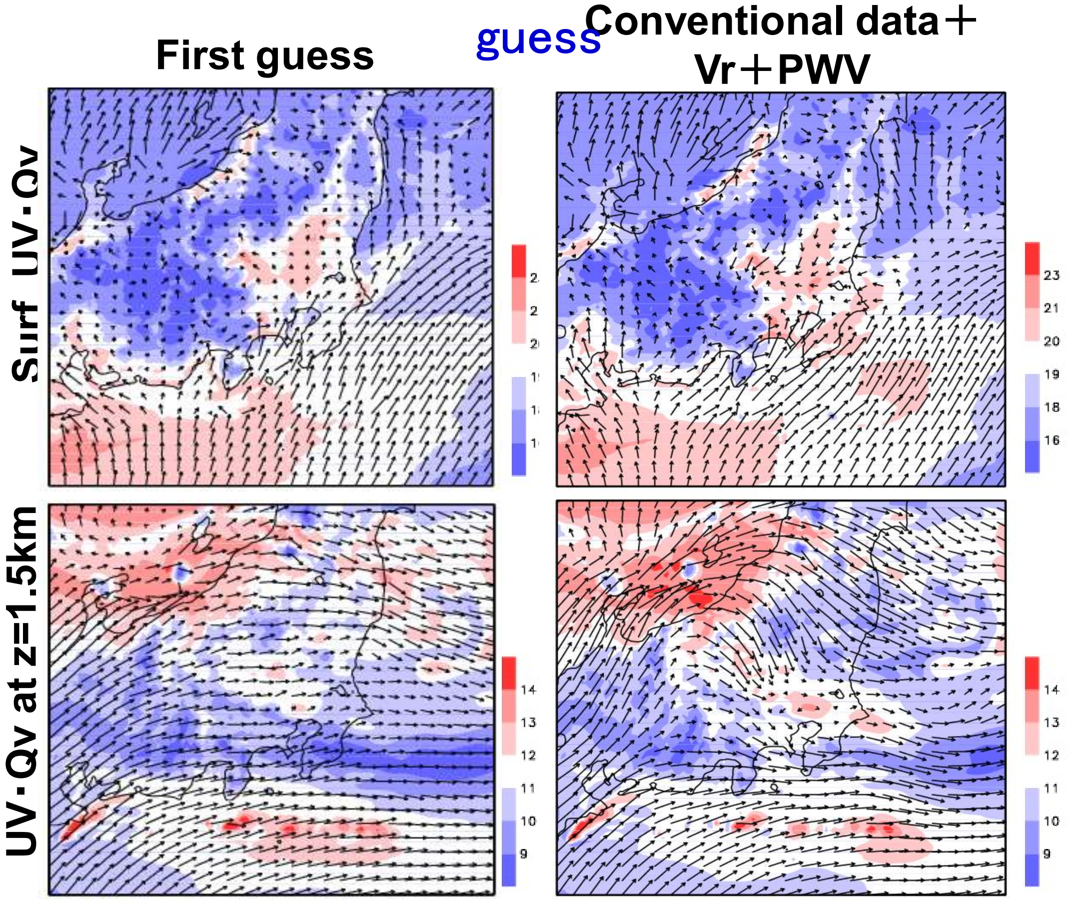

NHM-3DVar Forecast from Meso-4DVar results

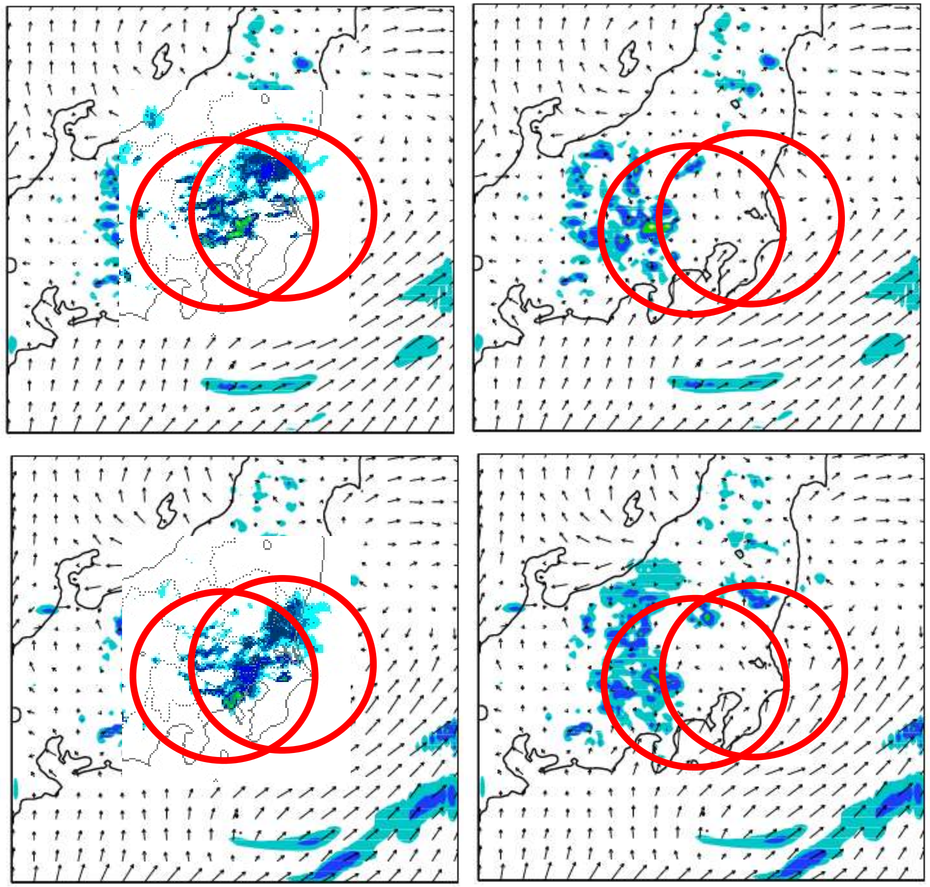

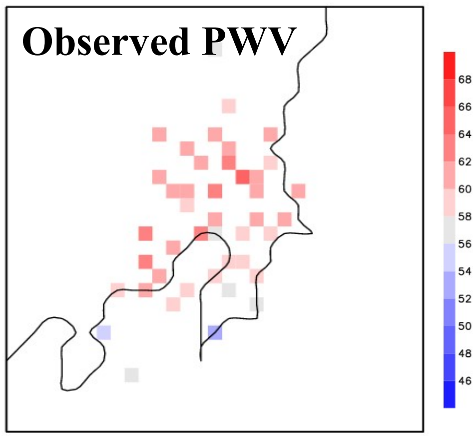

- When the PWV and Vr were assimilated, the northerly wind and moist inflow was reproduced.
- However, the precipitation was not reproduced at Kanto region.
- The horizontal interval of GPS station was about 25km.
- This interval was too long to express the convective scale water vapor distribution.

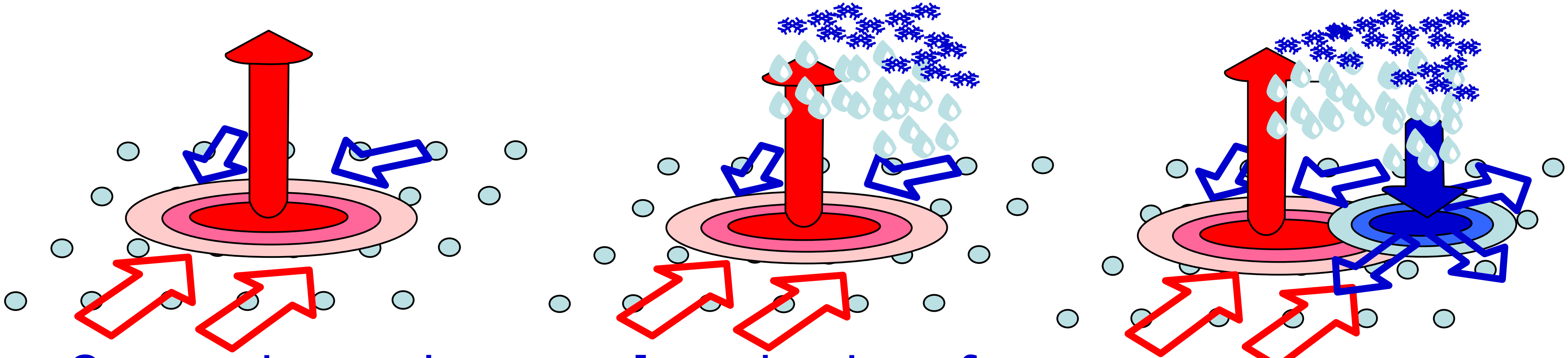

Convective scale water vapor

Updraft was moistened by relation between updraft and relative humidity.

Introduction of precipitation

Precipitation weaken the updraft. (One of features of decaying convection).

Unsaturated downdraft

Evaporation in downdraft produces intense outflow.

Relation between Updraft and RH within rainfall area

RH in precipitation regions was set according to the relation of 'RH' and 'w' (red line in the right panel).

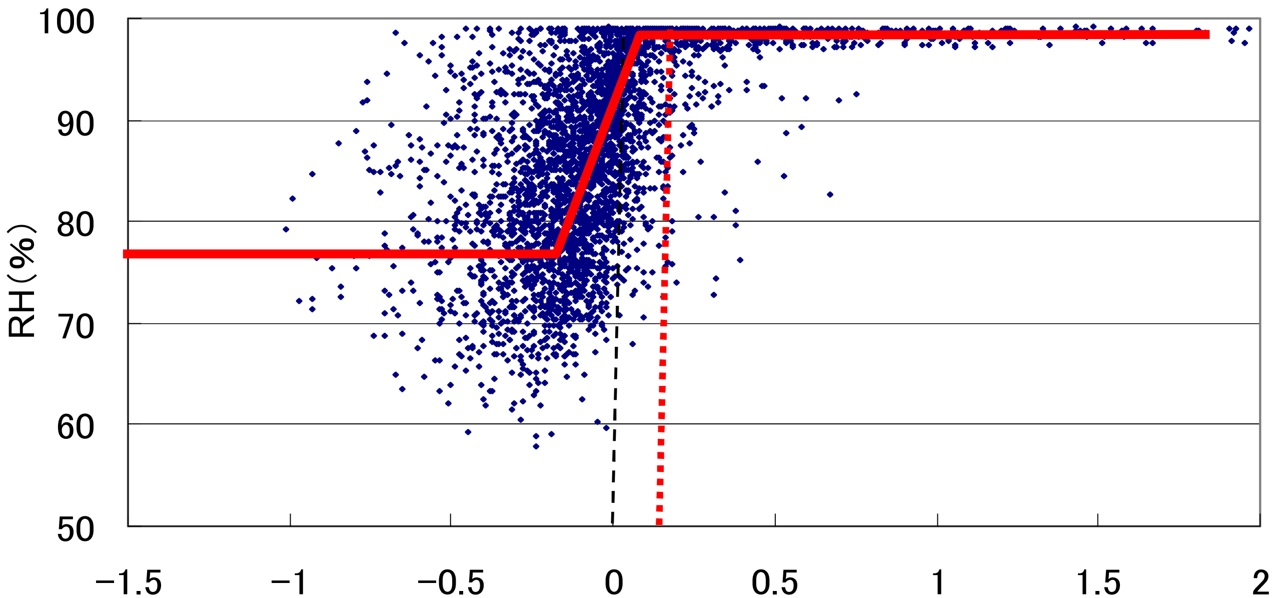

Scatter gram from simulated data of 12JST initial experiments.

Effect of convective scale water vapor

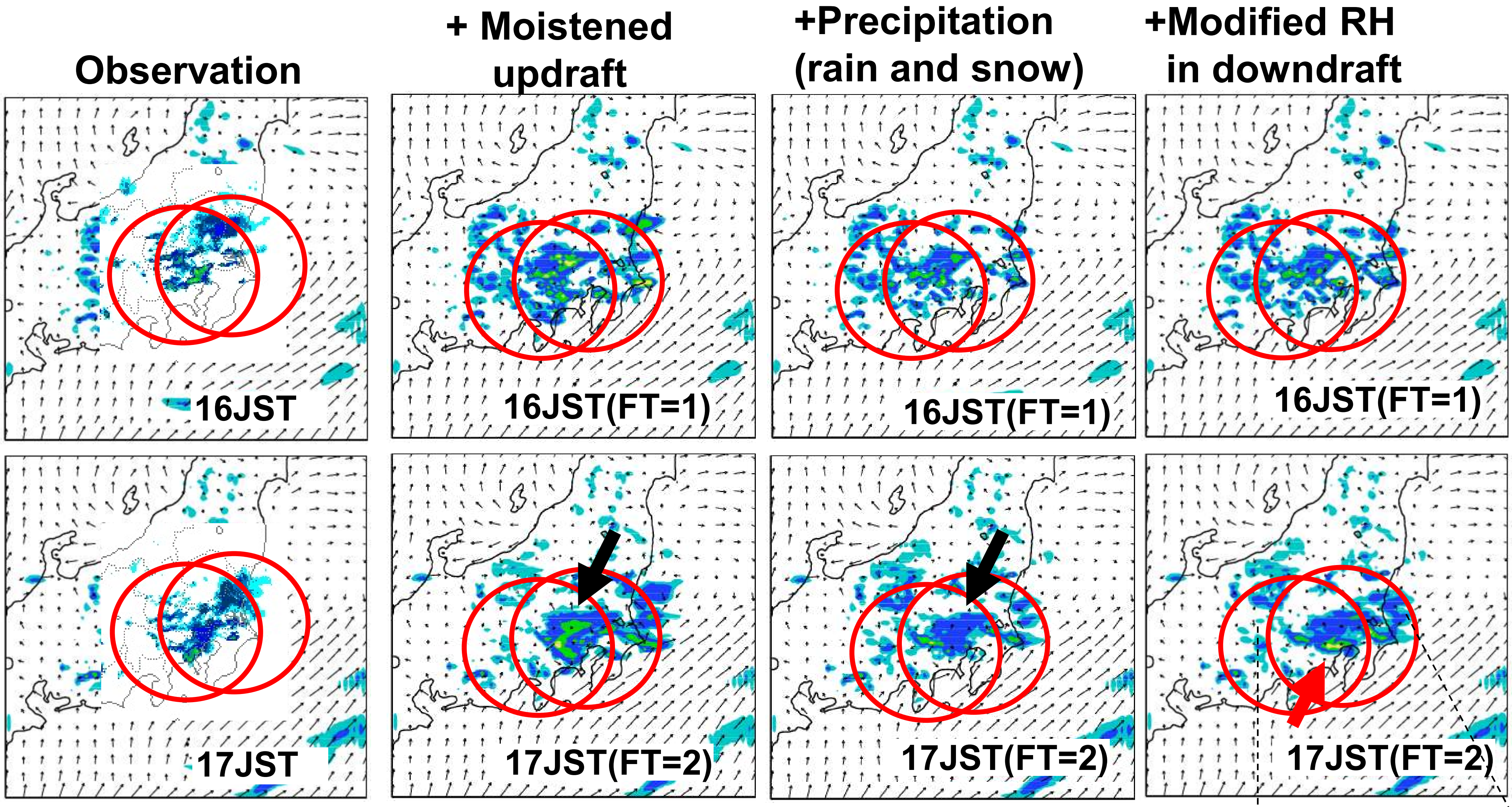

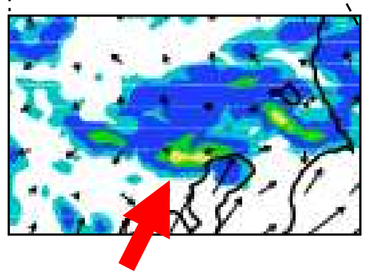

When updraft regions were moistened,

⇒Distribution of convection became close to observed one.

When precipitation and relation of RH and w were introduced,

⇒Decaying convection was reproduced (➡).

⇒Development due to outflow was also reproduced (➡) .

Simulated precipitation with NHM (Δx=2km)

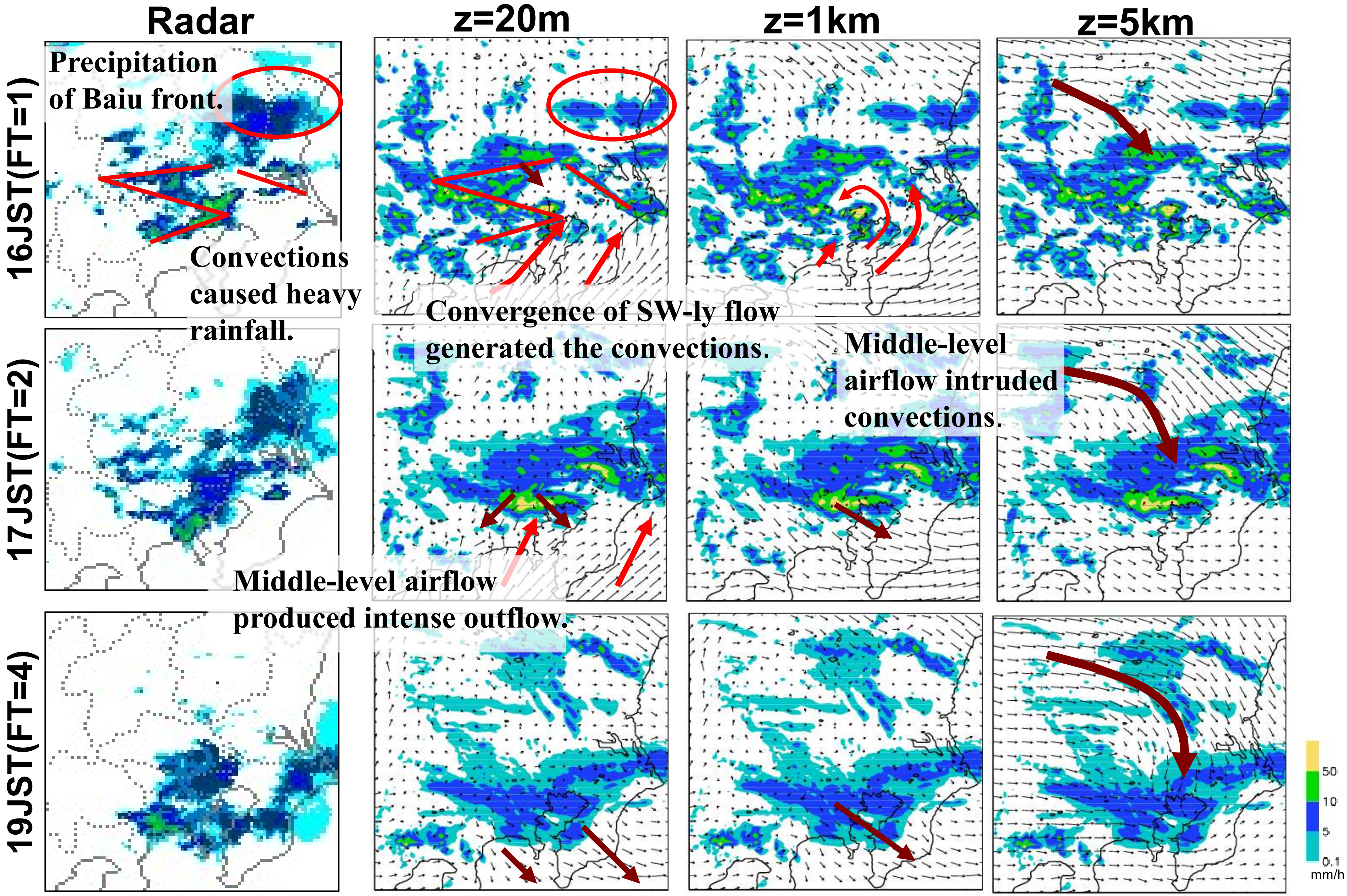

PT simulated with NHM (Δx=2km)

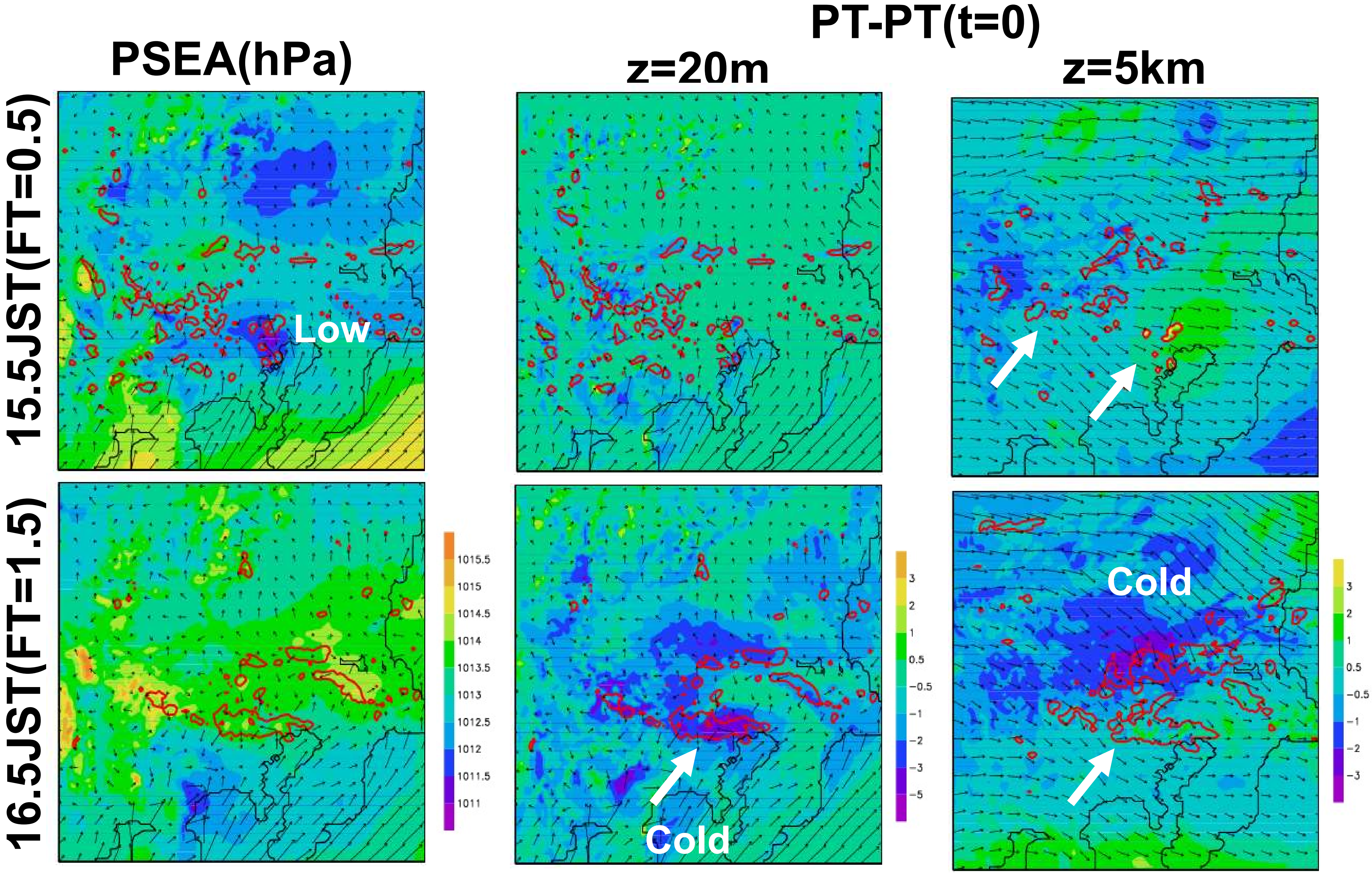

Qv simulated with NHM (Δx=2km)

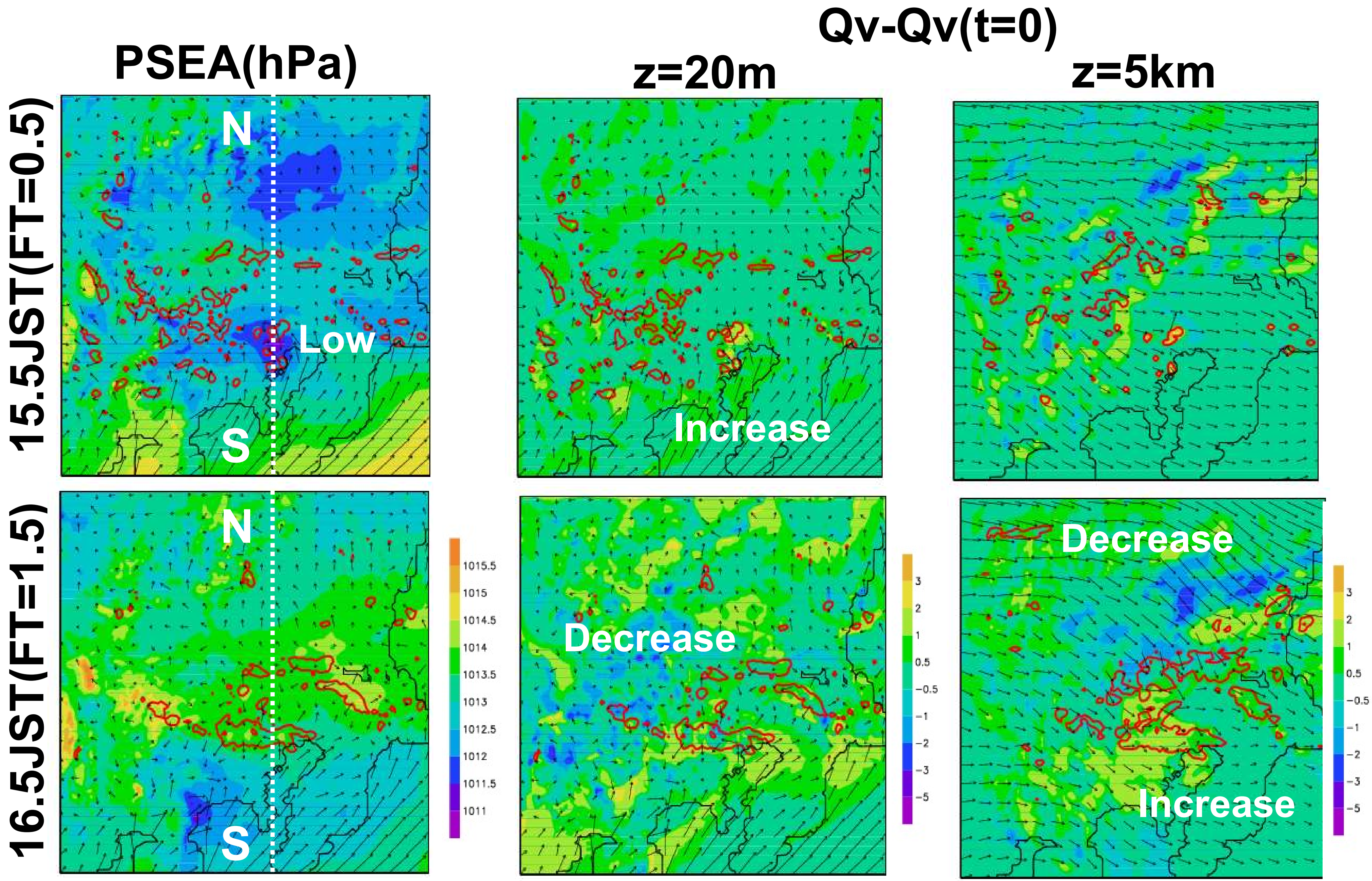

Vertical cross section of PT and Qv（Δx=2km)

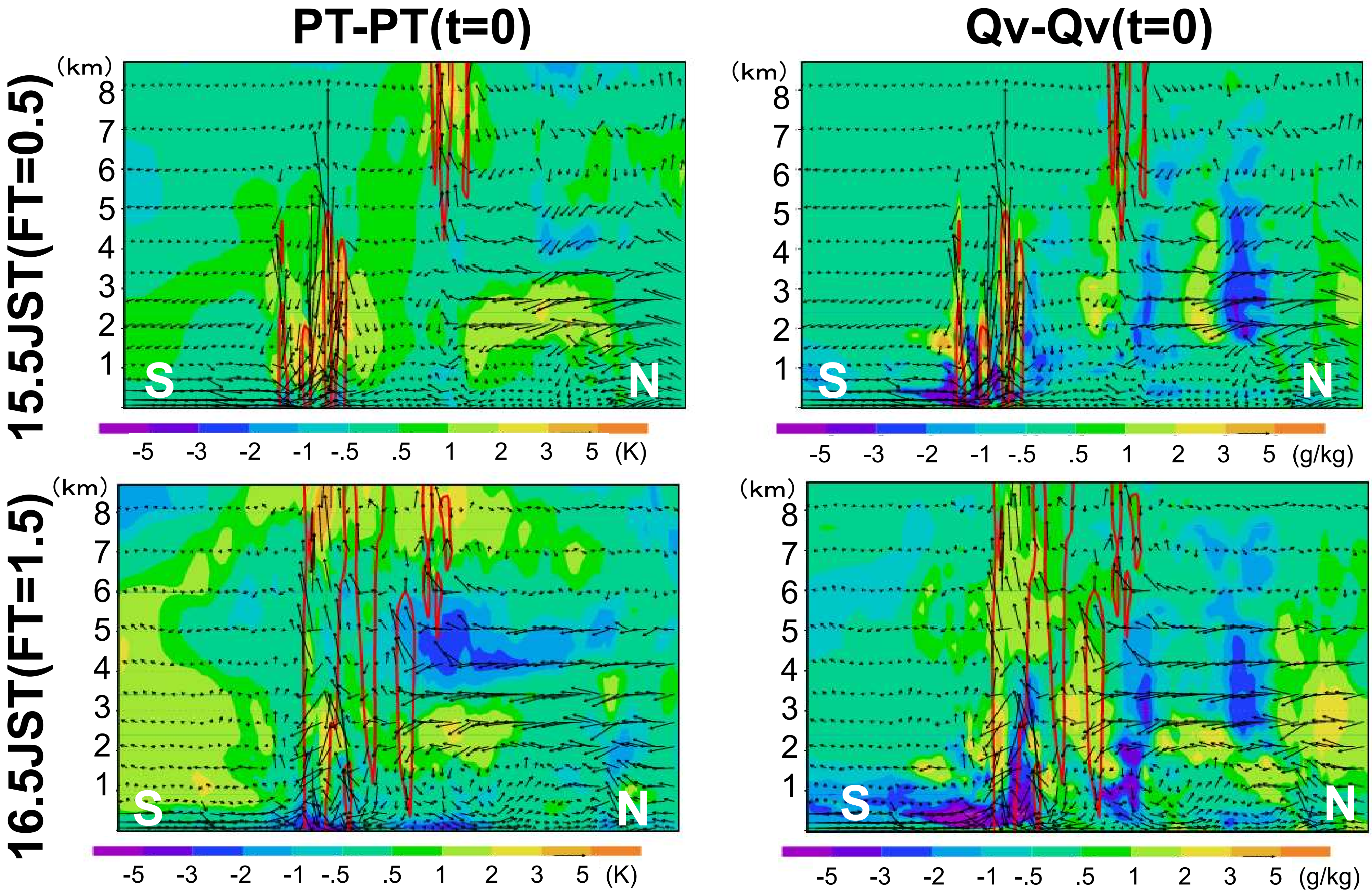

・Convections of heavy rainfall were generated before the arrival of cold dry air at middle level.

Summary

1. Doppler radar radial wind and GPS water vapor are useful data for the short-range forecast of the heavy rainfall.

2. Introducing of convective scale water vapor and precipitation help reproduce the heavy rainfall with NHM

3. The more realistic vertical profile is analyzed, when SWV was assimilated.

4. In this heavy rainfall case

There are 2 stages in the development of the heavy rainfall

(1) Convergence of humid low-level inflow generated the heavy rainfall .

(2) Middle-level cold rear inflow enhanced the heavy rainfall.

Thank you

Acknowledgements

The authors thank Dr. Y.-H. Kuo, Dr. T. Iwabuchi and member of COSMIC / University Corporation for Atmospheric Research, Mr. Y. Shoji and members of GPS/MET Japan project, for providing the useful comments and suggestions.

Our thanks extend to Drs. K. Koizumi, T. Miyoshi, S. Nishijima, Y. Ishikawa, K. Akaeda of JMA, Mr. Y. Tanaka and the staff of GSI for providing data assimilation programs, Doppler radar data, the decode programs of the Doppler data and GPS data.